Summer 1998

# An Injection Modelocked Titanium-Sapphire Laser

James C. Hovater
*Old Dominion*

# AN INJECTION MODELOCKED TITANIUM-SAPPHIRE LASER

by

James C. Hovater
B.S. May 1986, University of Maryland

A Thesis submitted to the Faculty of
Old Dominion University in Partial Fulfillment of the
Requirement for the Degree of

MASTER OF SCIENCE

ELECTRICAL ENGINEERING

OLD DOMINION UNIVERSITY
August 1998

Approved by:

Hani E. Elsayed-Ali (Director)

Sacharia Albin (Member)

Amin N. Dharamsi (Member)

# ABSTRACT


AN INJECTION MODELOCKED TITANIUM-SAPPHIRE LASER

James C. Hovater
Old Dominion University, 1998
Director: Dr. Hani E. Elsayed-Ali

I have investigated the possibility of using an injection modelocked Ti-sapphire laser as a illumination source for GaAs photocathodes. A commercial Ti-sapphire laser was modified to accept a seed pulse from a gain-switched diode laser. Modelocked operation was obtained through gain modulation within the Ti-sapphire crystal as a result of injection seeding with a modelocked pulse train from a gain-switched diode laser. The Ti-sapphire laser essentially becomes a pulse amplifier for the diode laser. Unlike conventional modelocked lasers, the pulse repetition rate of this laser can be discretely varied by setting the seed laser repetition rate equal to multiples of the Ti-sapphire laser cavity axial mode frequency. Pulse repetition rates from 223 MHz (fundamental) to 1560 MHz (seventh harmonic) were observed with an average output power of 700 mW for all repetition rates. Pulsewidths ranged from 21 to 39 ps (FWHM) under various pump laser conditions. This thesis includes: a survey of the state of the art in photocathode drive lasers, a qualitative description of injection modelocking, an experimental description of the injection modelocked Ti-sapphire laser, and measurements concerning pulse to pulse timing jitter and pulsewidth.

Co-Directors of the Advisory Committee: Dr. Matthew Poelker

This thesis is dedicated to my wife Lisa and
my children Tori, Sam and Anna.

# ACKNOWLEDGEMENTS

I would like to thank the following people who have contributed to the successful completion of this thesis. Matt Poelker for guiding me in an area of electrical engineering that I knew very little. Chris Cuevas for assisting in the collection of data. Dr. Hani Elsayed-Ali for allowing me to do my thesis at Jefferson Lab. My parents J. D. and Marilyn Hovater for pushing me to get my masters degree.

# TABLE OF CONTENTS

# LIST OF FIGURES

# CHAPTER 1

# INTRODUCTION

*Ti-Sapphire Lasers*

Ti-sapphire ($Ti:Al_2O_3$) was first proposed as a medium for a laser by Moulton [1.1]. He demonstrated a pulsed Ti-sapphire laser operating between 660 nm and 986 nm. A room temperature Ti-sapphire laser was soon built using a three mirror folded cavity, demonstrating the utility of such a laser [1.2]. A Ti-sapphire laser has also been built using a ring cavity [1.3]. In 1989 Alfrey built a four mirror folded cavity Ti-sapphire laser similar to the laser used for this thesis [1.4]. Since the late 1980's Ti-sapphire lasers have seen an explosion in growth. They have been available commercially for almost 10 years. Two reasons for this are this laser's broad fluorescent band that allows lasing from 700 nm to 1000 nm and its large linewidth (~ 40 GHz) that allows for ultrashort pulses (~ 1 ps). The absorption transitions occur between 400 and 500 nm, peaking around 500 nm, allowing for many types of pumping schemes. Ti-sapphire lasers can either be flash-lamp pumped or end pumped with either a argon-ion or doubled Nd-YAG. Typically, though, they are end pumped with another laser due to their relative short fluorescent lifetime of approximately 4 μs.

Of interest to Thomas Jefferson National Accelerator Facility (Jefferson Lab) and other electron accelerators around the world is that the optical wavelengths of the Ti-sapphire laser fall within the bandgap of GaAs a material used for polarized electron

sources (photocathodes). To eject electrons from the GaAs wafer a laser of some sort is needed. Ti-sapphire lasers operated cw have been used to illuminate GaAs sources [1.5]. They have the advantage of higher power and the optical frequency is easily adjusted. Recently investigations at Jefferson lab and Mainz in Germany have begun exploring the possibilities of using a modelocked Ti-sapphire laser [1.6, 1.7]. The Jefferson Lab laser is injection modelocked laser and acts as a pulse amplifier for a gain switched diode laser.

*Polarized Electron Sources*

Polarized electrons are required in a wide variety of physics experiments ranging from nuclear physics experiments involving the studies of quarks and the basic structure of the atom to atomic physics involving studies of solid surfaces [1.8]. At Jefferson Lab approximately half of the proposed nuclear physics experiments require polarized electrons. These electrons originate from a laser-driven photo-emission electron gun referred to as the photocathode. In most accelerators where electron polarization is a concern the photocathode material is GaAs [1.9].

The GaAs polarized sources require the use of a pump laser to excite the electrons out of the valence band (1.5 eV/850 nm). The electrons are polarized because of the spin-orbit splitting in the valence band of GaAs [1.10]. When the illuminating laser is circularly polarized angular momentum selection rules require that the positive or negative spin of the electron be determined by the light (polarization) angular momentum direction. Since the electrons can easily be polarized optically by switching the

polarization of the illuminating laser with a Pockel's cell, GaAs photocathodes have a great advantage over other sources.

*Existing Polarized Sources*

A photoinjector is designed as either dc or pulsed, which also essentially determines the type of illuminating laser used. In most accelerator applications a pulsed photoinjector is the preferred method, for a number of reasons. One reason is the need to synchronize the emitted electrons with the accelerating cavities. The photocathode needs to be pulsed at the accelerating cavity frequency or at a subharmonic in order for the electrons to be captured and accelerated. By pulsing at the accelerating cavity frequency, additional electron beam conditioning components like RF bunching and chopping cavities can be eliminated. In addition, pulsing the photocathode insures that all of the emitted electrons are accelerated and delivered to the ultimate user of the beam. None are wasted, as is the case when a DC laser light source is used to create a DC beam of electrons that must be chopped (in a manner similar to that of an optical chopper) and bunched prior to relativistic acceleration. An important aspect of this is that by using pulsed lasers the effective lifetime of the photocathode is prolonged as has been demonstrated at Mainz [1.7]. Accelerators using a pulsed photoinjector include Jefferson Lab, MIT Bates, and Mainz [1.11, 1.12, 1.13, 1.7]. In addition to existing accelerators, next generation accelerators such as the TESLA project (Next Linear Collider) are proposing to use polarized electron sources [1.14]. In addition free electron lasers (FELs) can utilize the high brightness beams that photocathodes can provide [1.15].

*Laser Systems*

The number of electrons produced is controlled by the power of the illuminating laser and the quantum efficiency (QE) of the photocathode. Thus it is in the interest of the gun designer to maximize the QE of the photocathode and to illuminate it with a laser with high average power. Many systems rely on a modelocked dye, or solid state, laser to energize the electrons. Either provides high average power, and both are very reliable. This method is fine if the accelerator is pulsed and has a repetition rate below 100 MHz since modelocked systems are limited below this frequency; accelerators such as the Continuous Electron Beam Accelerator Facility (CEBAF) at Jefferson Lab or Mainz require repetition rates up to 1500 MHz. The laser system used at CEBAF is a pulsed diode seed laser and semiconductor diode optical amplifier [1.11]. The laser system can be pulsed easily at either 499 MHz or 1497 MHz to deliver electrons to one or three users respectively. Since the system uses a dc biased laser diode, macro pulses can be created electrically instead of optically. The maximum average output power is 500 mW.

To get higher powers and therefore more electrons it is necessary to investigate solid state lasers, specifically Ti-sapphire. Ti-sapphire has become a popular choice for many short pulse laser applications. It can lase over a large wavelength range (650 nm to 1100 nm), deliver average powers up to 3 W, and easily meet pulsewidth requirements of tens of ps. It can also be used in various amplifier configurations such as regenerative, multi and single pass. Other accelerators are also investigating a Ti-sapphire. At the Mainz Microtron researchers have constructed a Kerr lens modelocked (KLM) Ti-sapphire laser capable of repetition rates of 1.2 GHz [1.7]. The Stanford Linear Collider

(SLC) is using a pulsed Q-switched Ti-sapphire laser to meet optical pulse energy requirements [1.16].

Jefferson Lab is investigating an injection modelocked Ti-sapphire laser to obtain higher power and faster repetition rates [1.6]. The laser is seeded by a gain-switched diode laser and the gain inside the Ti-sapphire laser cavity is effectively controlled by the modelocked pulse train from the diode laser. The modelocked Ti-sapphire laser effectively acts as a pulse amplifier for the diode laser. The pulse repetition rate of the seed laser is adjusted such that it is at the fundamental frequency (or multiple) of the Ti-sapphire laser cavity. The Ti-sapphire laser has been modelocked from a repetition rate of 233 MHz up to 1560 MHz, far beyond the limits of active or passive modelocking. The average output power for all repetition rates was approximately 700 mW.

This thesis investigates an injection modelocked Ti-sapphire laser system. Chapter 2 is a survey of existing photocathode laser systems and is used to provide background and comparative techniques. Chapter 3 qualitatively describes and compares the injection modelocking to injection locking and traditional modelocking. Chapter 4 discusses the operation of the injection modelocked Ti-sapphire laser. Chapters 5 and 6 discuss the phase noise and pulsewidth measurements conducted. Finally there is a brief summary of the major findings of the thesis.

# CHAPTER 2

# SURVEY OF EXISTING PULSED PHOTOINJECTOR LASERS

In last 20 years many different accelerator laboratories have begun using photocathodes to generate electrons. Depending on the needs of the accelerator the laboratories used different laser schemes to energize the electrons into the vacuum. The following is brief description of the different laser systems in use. Some of the methods to improve phase and amplitude noise are explained in detail to help the reader understand the significance of the measurements performed on the Ti-sapphire laser discussed later in the thesis. Both amplitude and phase effect the electrons coming off the photocathode and if these effects are not controlled properly beam requirements (bunchlength and energy spread) for the accelerator may not be met.

*Mainz Kerr Lens Modelocked Laser*

A group at the Mainz electron accelerator in Germany has developed a self-starting Kerr lens modelocked (KLM) Ti-sapphire laser to illuminate their GaAsP photocathode [2.1]. The design intention is similar to Jefferson Lab's in that they are looking for a more powerful pulsed laser system to extend photocathode lifetime and one that can operate at repetition rates above 1 GHz. The laser operates at 800 nm with a repetition rate of 1.039 GHz. Pulses of 210 ps FWHM have been measured with an average power of 520 mW using an argon-ion pump laser operating at 6.2 W.

Kerr lens modelocking is an established technique for creating ultrashort laser pulses [2.2 – 2.4]. It is based on the nonlinear self-focusing effect occurring in an

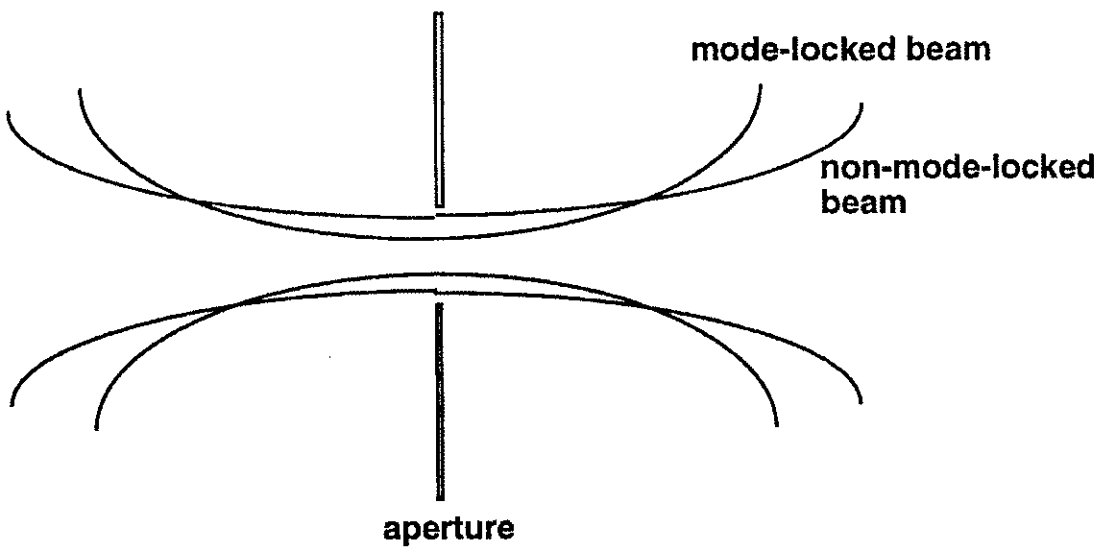


Figure 2.1 Self-focusing effects around a Kerr aperture inside a laser for a modelocked beam and non-modelocked beam. Together the aperture and the self-focusing are similar to a fast saturable absorber [2.3].

intracavity Kerr medium. The easiest way to create a nonlinear condition inside a laser cavity is with a simple aperture [2.3]. The way this works is shown in figure 2.1 [2.3]. If the aperture is placed in an appropriate position, a low power cw mode suffers large diffractive losses as it passes through the aperture. As the beam intensity increases the mode begins to focus down. The higher intensity pulse experiences lower loss and higher round trip gain than its low intensity counterpart. In effect the combination of the aperture and the self-focusing acts as a fast saturable absorber.

A problem for KLM lasers is that they do not instantaneously start to modelock; i.e., they need to have an initiating device to start the process. The Mainz laser overcomes this with a laser design such that nonlinear mode variation and the dynamic loss modulation are maximized [2.2]. In this way the laser essentially becomes self starting and no external or internal perturbations are necessary.

Figure 2.2 shows a diagram of the Mainz laser [2.1]. The design is a folded z geometry using an end pumped Ti-sapphire crystal. The crystal is cooled with a Peltier element. KLM is achieved by placing a vertical slit in front of the output coupler. To compensate for group velocity dispersion a thin glass etalon is placed in front of the reflecting mirror. The dielectric end mirrors are coated for center wavelength of 800 nm and wedged to minimize reflections. The output coupler is designed for 5% transmission.

The laser operates reliably up to pump powers of 6.2 W corresponding to 520 mW of average output power. As the pump power was increased to 11 W an output power of

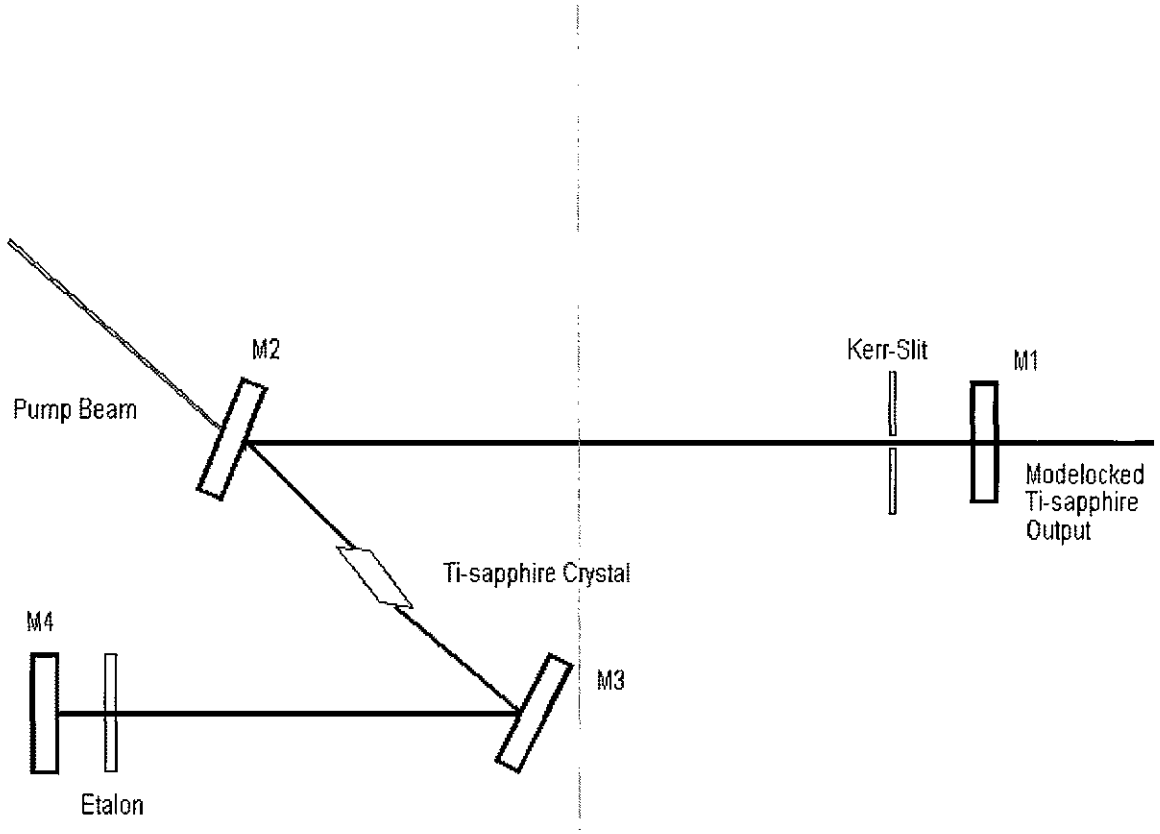


Figure 2.2 Diagram of the Mainz Kerr-lens Ti-sapphire modelocked laser [2.1].

950 mW was obtained briefly before thermal lensing in the Ti-sapphire crystal stopped the lasing. Additional cooling on the crystal did not solve the problem. They have observed at least five longitudinal modes up to 4.156 GHz that are phased locked, which corresponds to an FWHM pulsewidth of 210 ps. Presently the pulsewidth limitation is due to the glass etalon which can only compensate over a few GHz.

*The Jefferson Free Lab Electron Laser Photoinjector Drive Laser*

At the Jefferson Lab free electron laser a commercially available Antares$^{TM}$ (Coherent Inc.) frequency doubled (527 nm) Nd:YLF laser is used [2.5]. Unlike the polarized sources for nuclear physics, FELs need high peak currents to increase the power gain within the FEL. The Jefferson Lab FEL also uses a GaAs photocathode, but to increase the quantum efficiency the drive laser is frequency doubled such that the photon energy is far beyond what is needed to remove electrons from the valence band. The laser is actively modelocked to the 20$^{th}$ subharmonic of the accelerator cavity frequency (1497 MHz). The laser can deliver 45 ps FWHM pulses and 5 W average power reliably at the second harmonic (527 nm). The laser system is shown in figure 2.3. The laser is flash lamp pumped and generates 1054 nm at an approximate average power of 20 W. The Nd:YLF is actively modelocked in the classical way with an active acoustic-optical modelocker [2.6].

An important aspect of the laser is that it must meet stringent phase and amplitude jitter specifications. To achieve this the laser is phase locked to a master reference by using a portion of it as the drive signal to the laser modelocker (1497 MHz). In this way

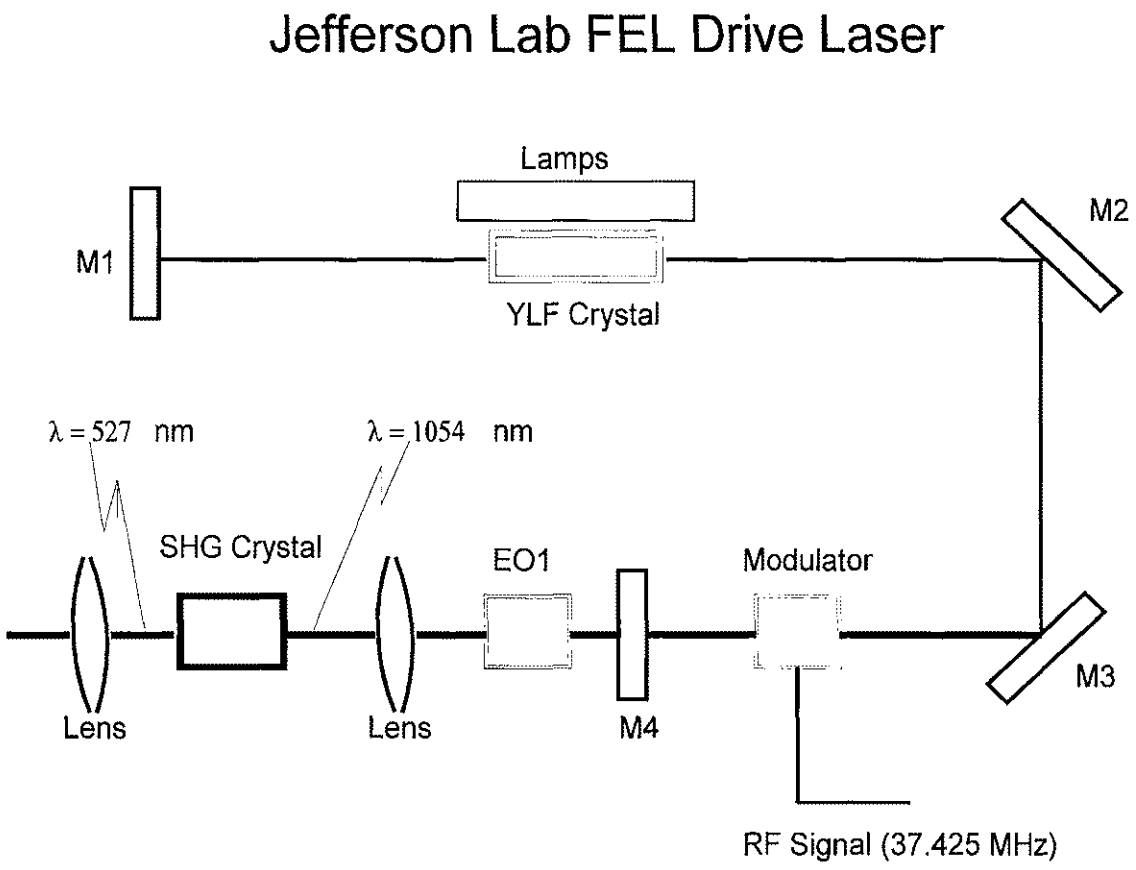


Figure 2.3 Diagram of the Jefferson Lab FEL photocathode drive laser [2.5].

the phase of the electrons can be controlled and synchronized with the accelerating cavities. The phase of the laser pulse train is actively controlled by comparing the $20^{th}$ harmonic of the laser pulse to the master oscillator and correcting on the error. This minimizes any phase changes that might occur from the laser cavity's length changing. The rms phase jitter at 1497 MHz is $< 1^{\circ}$ or 2 ps [2.5]. The laser has been reliably driving an operational photocathode since January of 1997.

*Laser System for the TESLA Photoinjector*

A similar laser system to the Jefferson Lab FEL drive laser has been built for the TESLA collaboration. TESLA is a collaboration of laboratories and universities that are proposing to build a next generation electron collider using superconducting RF technology. The laser system produces a 1 MHz train of up to 800 equal amplitude pulses with up to 800 mJ per pulse at $\lambda = 1054$ nm [2.7]. The laser is a phase stabilized, modelocked Nd:YLF oscillator. The pulse train is produced by a fast selection Pockel's cell. The pulses are then amplified through a series of multipass Nd:glass amplifiers. To produce the required 10 ps pulses the system employs chirped pulse amplification using an optical fiber and grating compressor. Finally the pulses are passed through two SHG (second harmonic generator) crystals to produce a wavelength of $\lambda = 263$ nm. Unlike the GaAs photocathode systems discussed previously, the TESLA project is using a $Cs_2Te$ based photocathode cathode which requires UV radiation to energize the electrons. A block diagram of the system is shown in figure 2.4 [2.7].

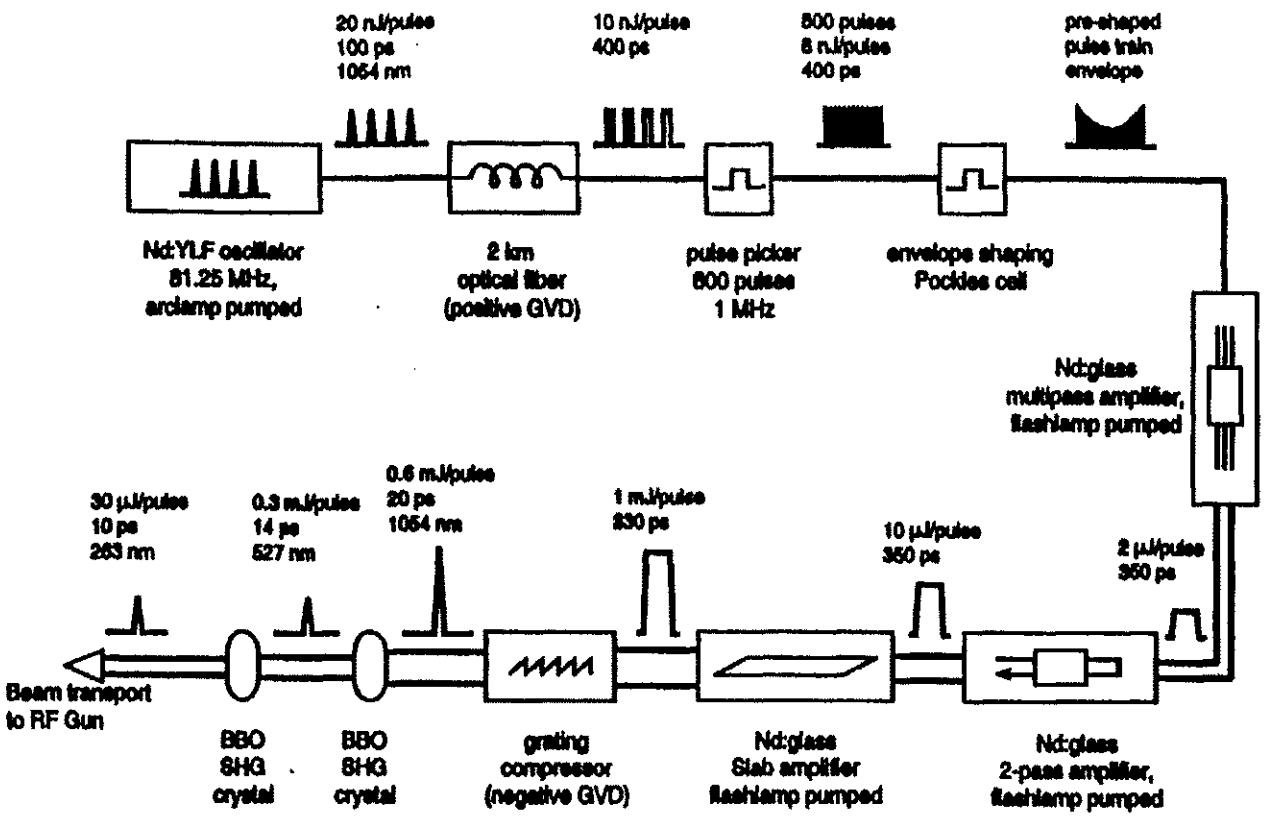


Figure 2.4 Schematic of the TESLA photoinjector drive laser [2.7].

Like the Jefferson lab FEL drive laser, the TESLA laser is referenced to a master oscillator which drives the superconducting accelerating cavities. Similarly the phase of the modelocker is controlled through feedback to enhance the phase stability with respect to the master oscillator. They use a commercial system (Lightwave model 1000) to phase lock the laser, while the Jefferson Lab system uses a modified accelerating cavity phase controller. With this system timing jitter is below 2 ps rms, which compares favorably with the Jefferson Lab FEL laser and the Ti-sapphire laser reported here.

A challenge for the designers was that each pulse had to have the same energy as the previous pulse. The reason for this is that the accelerating cavities require a constant electron current to maintain proper acceleration. Since the electron bunch charge is proportional to the laser energy, the laser has to be stable. To ensure that the pulses are approximately identical in energy, the laser amplifiers have custom designed power supplies which provide constant current discharge to the flashlamps for > 800 μs. An additional energy correction is made by preshaping the profile of the injected micropules by means of an amplitude modulating Pockel's cell. Shot to shot variation (small changes in optical alignment) in the amplifiers is also of concern, especially since they are not operated at saturation. To minimize these effects the amplifiers are operated with high gain and fewer passes. The designers are also investigating an adaptive feedback system to produce a best average correction shape.

Pulse compression is needed to adjust the output for the needed 10 ps pulse. Short, high energy pulses can be produced using chirped pulse amplification (CPA). The pulses

are stretched in time and swept in frequency, "chirped", by propagating them through a long optical fiber, 2 km. This also has the added benefit of allowing the pulse to be pre-shaped for energy stability more easily than with a short pulse. After amplification the chirp is reversed by adding negative group velocity dispersion using a pair of parallel diffraction gratings. Since the process of each harmonic generation reduces the pulsewidth (FWHM) by the square root of 2 the diffraction gratings are adjusted for an IR pulsewidth of 20 ps. The SHG crystals are identical BBO crystals. The conversion efficiency is approximately 50% for the second harmonic and 10% for the fourth harmonic.

*The SLAC Photoinjector Drive Lasers*

The Stanford Linear Collider (SLC) has used Ti-sapphire lasers in two variations. One is end pumped with an Nd:YAG (neodymium-doped yttrium aluminum garnet) laser and the other is flash lamp pumped [2.8]. The reason for the latter is that the Nd:YAG pumped system could not provide the required 2.2 μs pulsewidth needed for a particular nuclear experiment due to the short excited state lifetime of Ti-sapphire (~ 4 μs).

The Nd:YAG pumped system uses a Q-switched and cavity dumped Ti-sapphire laser to energize polarized electrons from a GaAs photocathode [2.9]. Figure 2.5 shows a block diagram of the laser system. The laser produces an energy of 50 μJ with a required 2 ns double pulse at a 120 Hz repetition rate. The laser operates at wavelengths between 760 nm and 870 nm. Unlike the accelerators at CEBAF and Mainz, the SLC is pulsed and therefore the laser requirements are somewhat different. Here the photoinjector is looking

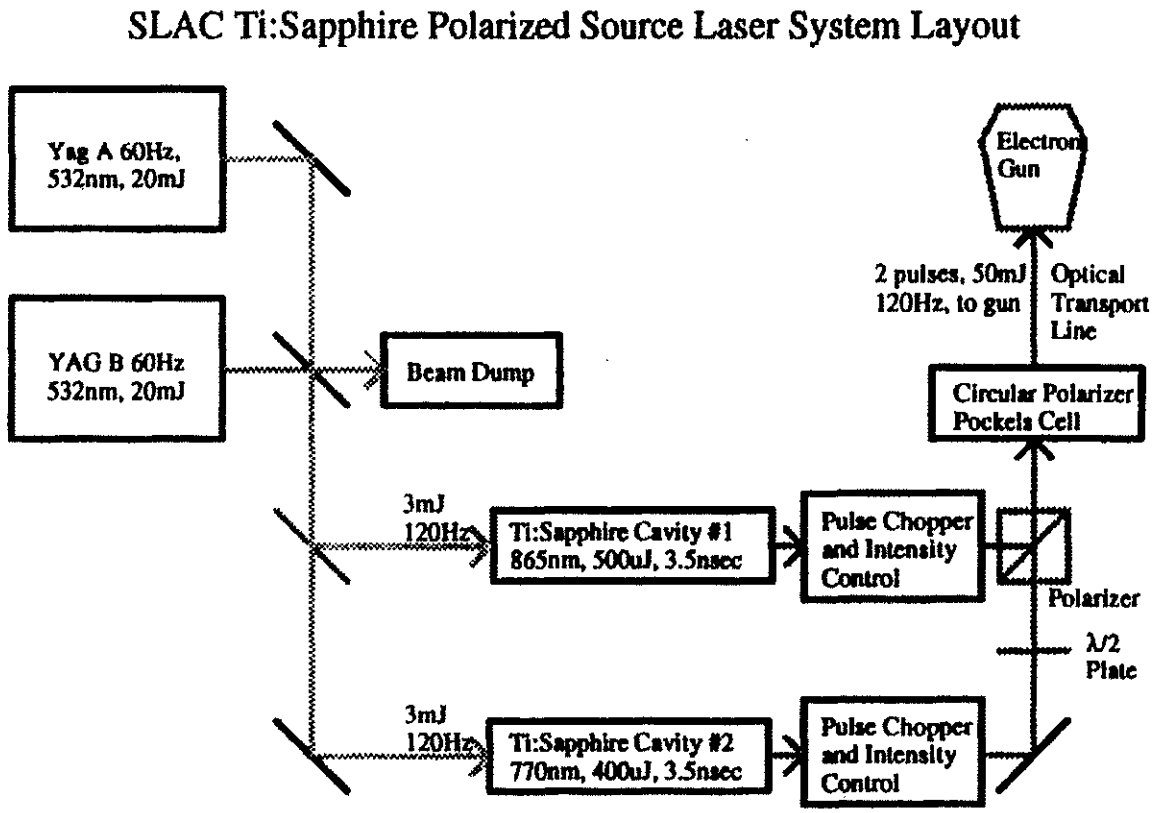


Figure 2.5 Diagram of SLAC polarized source drive laser [2.9].

at delivering peak currents in the range of mA vs. μA in a typical cw (CEBAF) machine. This is to make up for the lack of electrons delivered because of the pulsed operation. A unique feature of the laser is the requirement of two pulses (2 ns) separated by 62 ns. The pulses are required to generate the electron bunch and the positron bunch for the collider. To do this two Ti-sapphire laser cavities together with two pump lasers (frequency doubled Nd:YAG) are used to produce the pulses. This allows individual control of pulse timing and intensity.

The laser cavities are Q-switched and cavity dumped using an intra-cavity Pockel's cell and polarizer. By applying high voltage to the Pockel's cell, the polarization of the light in the cavity is rotated and lasing stops. When the high voltage is removed, light within the cavity begins to build up. Finally, when the optical power within the cavity has reached its maximum, a fast high voltage edge is applied to the Pockels cell which allows circulating light to be extracted through one of the polarizers. The pulse length is the round trip time of the cavity.

The pulse to pulse energy and timing are stabilized through a series of feedback loops. First the Nd:YAG flash lamp high voltage is controlled by a photodetector that monitors the output energy. The output power from the Ti-sapphire cavities is controlled by intensity feedbacks which detect the optical energy and control the high voltage to a Pockels cell. In addition the feedback loops monitor the buildup time of light in the cavity and control the stop time of the Q-switch pulse assuring the cavity dump time at the peak of the optical pulse. Timing is stabilized between the four lasers by separate timing

feedback loops. Lastly a fast feedforward system measures the Nd:YAG output energy and then adjusts the stop time of the Q-switch. The Intensity Jitter is reduced from 12% to < 3% with these systems. The intensity jitter is also neutralized by operating the photocathode above saturation, something other accelerators can not. Taking all this into account the current stability of the photocathode is < 1.6 % rms.

The flash-pumped Ti-sapphire laser uses a pair of short pulse flash lamps coupled to a Ti-sapphire rod with a dual elliptical specular reflector cavity [2.8]. Ti-sapphire is typically difficult to flashlamp pump given its short excited state and narrow absorption band centered around 500 nm. Increasing the flashlamp energy produces a hotter discharge, which pushes the spectrum farther into the UV but yield only a small increase in energy in the required band. Decreasing the pump pulse length unfortunately increases the discharge temperature ultimately reducing the flashlamp lifetime. To compromise between the two effects, SLAC designers settled on a 7.5 μs pump pulse. A 6 kV thyratron modulator was used for the flashlamp discharge circuit which was capable of providing 30 J. To get to the required 2.2 μs laser pulse a fast Pockels cell was used as a chopper. Similarly to the Nd:YAG pumped system feedback was used to stabilize the Pockels cell driver producing a laser intensity jitter of 2% rms and a square output pulse.

*The CEBAF Photoinjector Drive Laser*

The laser system presently used at CEBAF is a pulsed gain-switched diode seed laser and semiconductor diode optical amplifier [2.10]. The laser system can be pulsed at either 499 MHz or 1497 MHz to deliver electrons to one or three users respectively. The

pulsewidth is approximately 50 ps FWHM, which is ideally suited to deliver electron bunches that must pass through the injector chopping slits. The laser system is compact and efficient, rests on a table directly beneath the electron gun and requires no HV or water for cooling. Since the system uses a dc biased laser diode, macro-pulses can be created electrically instead of optically. The maximum average output power is 500 mW. Figure 2.6 shows a diagram of the CEBAF gain-switched diode with the semiconductor amplifier.

Gain-switched diode lasers offer many advantages over other laser sources [2.10]. They are simple, compact, and reliable sources of short pulse, high repetition laser light. The main advantage of gain-switching over modelocking is that the pulse repetition rate is determined solely by the diode drive frequency and not the cavity length, as in a conventional modelocked laser. Repetition rates up to multiple GHz are possible using such devices. This method also requires no intracavity elements making the system inherently stable. Pulse stability is only dependent on the electronic drive circuitry. While it is true that gain-switched diodes can not achieve pulsewidths much below 10 ps, this is not a requirement for its present application. A serious disadvantage for these devices is the low average output power, but this can be overcome when one is mated with a semiconductor or solid state amplifier.

Presently to overcome this problem the CEBAF laser seeds a GaAlAs tapered-stripe, traveling wave semiconductor amplifier [2.10]. For reasons similar to those in the case of the as the gain-switched diode, a semiconductor amplifier is more practical than

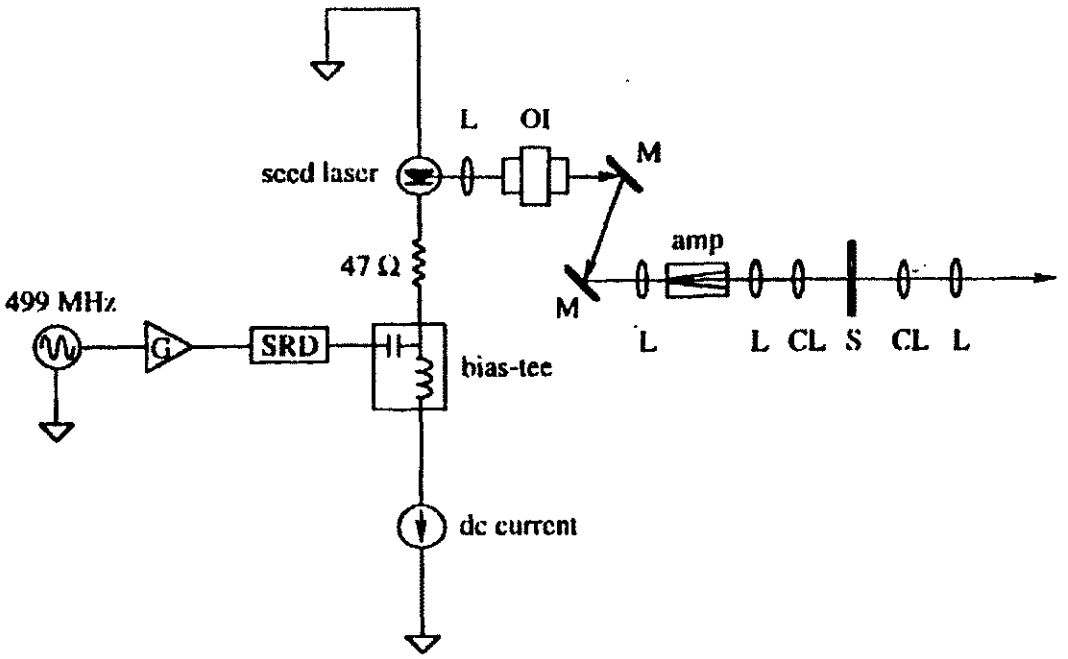


Figure 2.6 Diagram of the present CEBAF drive laser. The laser consists of a gain-switched diode laser and a semiconductor laser amplifier [2.10]. L, lens; OI, optical isolator; SRD, step recovery diode; CL, cylindrical lens; M, mirror; S, slit; G, amplifier.

other amplification sources. It is rather efficient electrically, requiring only a dc bias and a couple of amperes. Comparing it to solid state amplifiers, it does not need a pump laser or flashlamp, or the high voltage supply that may accompany them. The CEBAF laser system is limited to output power of 500 mW, which is less than a solid-state system can deliver. The advantages of using the gain-switched diode and semiconductor amplifier over other short pulse techniques presently outweigh the limited average power. Other accelerators, such as Athens Race Track Microtron and MIT Bates, are developing similar laser systems [2.11].

*Summary*

In general photoinjector lasers are designed around the photocathode material they intend to drive, since it is dependent on the electron bandgap energy. GaAs polarized sources in particular need lasers capable of wavelengths between 750 to 850 nm. Below this wavelength the polarization of the electrons decreases because of the narrow band splitting of the GaAs. Above the wavelength the required bandgap energy is not reached and electrons can not break free into the vacuum. The accelerators that have the most in common with the CEBAF polarized injector are Mainz and MIT Bates. Both are following similar paths (semiconductor diode amplifier and Ti-sapphire) to develop a drive laser.

An important aspect for any photocathode drive laser is energy and timing jitter [2.12]. Almost all drive laser systems use some kind of active feedback or feedforward compensation to reduce these effects. This is driven by the end users' (typically nuclear

and high-energy physicists) requirement for stable and repeatable electron bunches. Laser energy jitter will correlate directly to current fluctuations in the electron beam. Laser timing jitter (phase noise) will affect the absolute longitudinal bunch length of the electrons. Unfortunately this noise is seldom random (good) and usually associated with line harmonics (unchecked correlated noise can make a two month physics experiment useless!).

# CHAPTER 3

# INJECTION MODELOCKING

*Introduction*

A discussion of injection modelocking would not be complete without a discussion of traditional modelocking and injection locking. Injection modelocking can be considered a hybrid of both depending on how you define each. In this thesis I inject a modelocked diode laser pulse into a cw Ti-sapphire laser. The laser responds like a modelocked laser in that the pulses are a function of the laser cavity round trip time and the laser is operating close to the cw optical frequency and not that of the seed laser. The Ti-sapphire laser is phase locked to the RF signal pulsing the diode laser similar to an injection locked laser. Therefore a discussion of modelocking and injection locking is helpful.

*Traditional Modelocking*

Modelocking was first demonstrated almost simultaneously in the 1960's by a number of individuals [3.1]. The benefits from a modelocked cavity were seen immediately. Their extremely short optical pulses could be applied to many different areas of research including solid state physics, atomic physics and biology, especially where the dynamic time scales were faster than tens of picoseconds.

The method of modelocking a laser is fairly simple [3.1]. A laser cavity can oscillate at any of its axial modes as long as the gain can overcome the lasing threshold.

Typically the laser will lase across all axial modes unless the gain profile is narrow or some form of gain modulation is present to lock it to one particular mode. The optical light will consist of many pulses that are out of phase with one another. If only a few modes are oscillating, the output of the laser would have a periodic envelope similar to an FM signal. More often, though, especially in solid state lasers, the gain profile is broad and many out of phase pulses are present, making the envelope appear constant. If the laser gain inside the cavity is modulated at the cavity frequency, which is the time it takes for a photon to traverse the cavity and back (typically 10 to 100 MHz), then phase coherent single pulses will emerge at the cavity frequency. This contrasts with the case of a cw laser when all of the pulses within the cavity are not in phase.

There are two types of modelocked lasers: active modelocking, where the gain in the cavity is externally modulated by some sort of optical device, and passive modelocking, where a saturable absorber is placed in the cavity that allows pulses to become phase locked. In most cases these devices are limited to the bandwidth of the modulating device. In the case of the passive modelocked lasers (especially KLM lasers) cavity size becomes an issue above 1 GHz (at 1 GHz cavity size is 0.15 m), where small drifts in cavity lengths can cause problems. Presently many photocathode drive lasers are actively modelocked lasers [3.2, 3.3]. They typically operate at sub-harmonics of the accelerating cavities because they are limited by the laser cavity frequency.

*Injection Locking*

The concept of the injection locking of oscillators is well known and has been described at various lengths [3.4, 3.5]. A very good description of laser injection locking is given by C. J. Buczek et al. where they describe injection locking of CW $CO_2$ lasers [3.6]. Included under laser injection locking is regenerative amplification, which is the operation of a laser oscillator below threshold. A number of regenerative amplifiers using Ti-sapphire have been built [3.7, 3.8]. They can support only pulsed outputs (< 10 kHz) because of the regenerative process.

To injection lock an oscillator, a weak spectrally pure signal is injected into the resonant circuit of another self-sustaining oscillator (slave). The injected frequency must be close to that of the free running oscillator so it can capture or lock the subsequent oscillation behavior. The slave oscillator is then controlled by the injected "master" oscillator. If the frequency of the seed laser is detuned from the resonance of the slave oscillator, the output will follow the frequency of the externally injected laser. At some detuning range the externally injected signal can no longer force the slave oscillator gain below threshold, and other oscillator axial modes are allowed to exist, leading to multiaxial mode operation. It should be understood that it is the optical frequency that is being controlled and not the axial mode frequency of the slave laser.

*Injection Seeding (Pulsed Injection Locking)*

A hybrid of injection locking is the concept of injection seeding. Unlike injection locking, injection seeding can exert axial mode control within the laser cavity. A very

weak or far off resonance signal is injected into a high power pulsed laser oscillator during the turn-on period when the laser is building up from noise. As stated, the injected signal is too weak or far from resonance to lock the laser successfully. It can establish the initial conditions from which the oscillation will build and thus exert some control over the signal in the laser.

Injection seeding has been demonstrated using a number of different types of lasers. J. L. Lachambre et al, used a cw $CO_2$ master oscillator and a high power TEA-$CO_2$ laser [3.9]. Park and Byer have demonstrated injection seeding in pulsed Q-switched Nd:YAG laser oscillators [3.10, 3.11]. More recently Bair et al., injection seeded a Ti-sapphire ring laser with cw diode laser, in addition Barnes et al., demonstrated injection seeding using a Ti-sapphire unstable resonator [3.12, 3.13]. In both of the Ti-sapphire cases, the lasers were operated in pulse mode and the objective of injection seeding was as an amplification process for LIDAR. There was little interest and or need in creating short optical pulses and operating cw.

Figure 3.1 illustrates the axial mode selection process by injecting an external signal close to an axial mode of a laser oscillator [3.10]. The injected field leads to amplification of the axial mode starting at the seeded signal amplitude instead of from noise. Since the bandwidth of the injected signal is much narrower than the axial mode spacing, other modes are not influenced. Since one particular axial mode is given a gain advantage over the other noninjected axial modes, it will reach saturation, first extracting energy from the gain medium that would otherwise be used by the other modes, hence

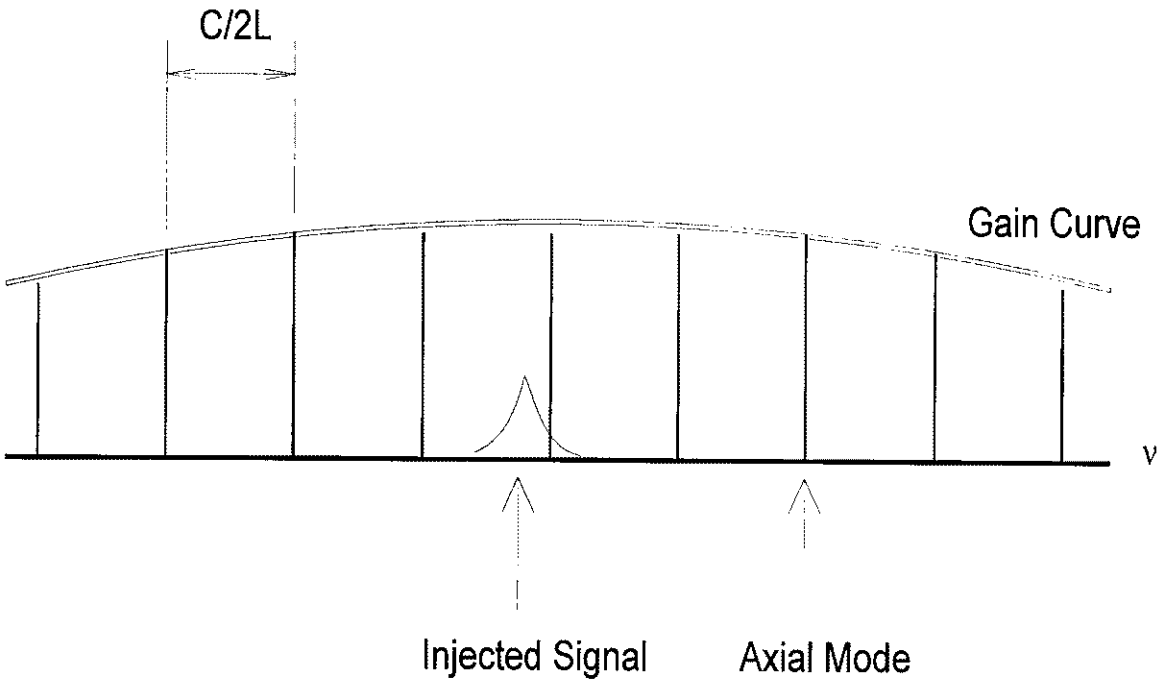


Figure 3.1 Diagram showing the how injection seeding selects a single axial mode [3.10].

single axial mode oscillation. When an external signal is injected into a high gain pulsed laser oscillator whose axial mode separation is much wider than the bandwidth of the injected signal, an axial mode selection process takes place instead of the optical frequency locking process. In injection seeding, laser oscillation occurs at the frequency near an axial mode, thereby determining the laser's repetition rate.

*Injection Modelocking*

A cw laser will typically have many axial modes that are not in phase. As mentioned previously, an intracavity modulator can be installed to synchronize the pulses and lock the modes together. Another method is to inject the laser with a modelocked pulse train which contains a large number of phase locked axial modes. This leads to a large number of axial modes in the laser cavity being excited in phase [3.15]. Within a few round trips the injected signal gives a gain advantage to the selected axial modes, allowing them to grow and uniformly saturate the gain. This produces an output containing a large number of phase locked axial modes, resulting in a short modelocked pulse. Like injection seeding, the injection modelocking requires that the injected signal needs be close to the axial mode frequency to obtain a modelocked pulse. Unlike injection locking, though, the lasers (seed and slave) do not have to have the same optical frequency.

The first instance of modelocking by injecting a modelocked pulse train into a laser was demonstrated by E. Moses et al. using a flash-lamp pumped dye laser injection locked to a modelocked dye laser [3.14]. They observed that with injecting 15 ps pulses

into the flash-lamp pumped dye laser they obtained 20 ps pulses out. In this case the wavelength of the slave laser was determined by the injected seed. An injection modelocked Q-switched Nd:glass laser was demonstrated by Basu in his Ph.D. dissertation [3.15]. The laser was seeded by a dye pumped modelocked Nd:glass laser producing a maximum average output power of 13 mW at pulse repetition rate of 174 MHz. The modelocked laser was directed into the Q-switched cavity through an optical isolator and a partial beam splitter. The output of the modelocked laser was spatially mode-matched to the lowest traverse mode of the Q-switched oscillator. When injected with 50 ps pulses from the modelocked laser, the output of Q-switched laser became a series of short pulses under the Q-switch envelope. There were 12 subpulses under the Q-switched pulse envelope of 69 ns FWHM. It was mentioned that the injected pulse width degraded only slightly (< 25%) as long as the cavity length mismatch was less than 0.2%. There was no mention of the optical frequency of the two lasers (seed and slave), but I assume they were close.

An injection modelock Ti-sapphire laser was also demonstrated by Basu [3.16]. Figure 3.2 shows a diagram of the experimental arrangement. The laser was pumped with Q-switched Nd-YAG laser, which was doubled to provide an energy of 122 μJ per 100 nsec-long pulse at 532 nm for pumping at a 1 kHz repetition rate. Injection seeding was accomplished using a single quantum well laser, which produced pulsewidths of 19.4 ps. The Ti-sapphire laser was tuned to match the 820 nm peak of the laser diode spectrum. When the laser diode output was spatially mode matched with the Ti-sapphire laser, the gain switched Ti-sapphire laser broke into a series of short pulses separated by the cavity

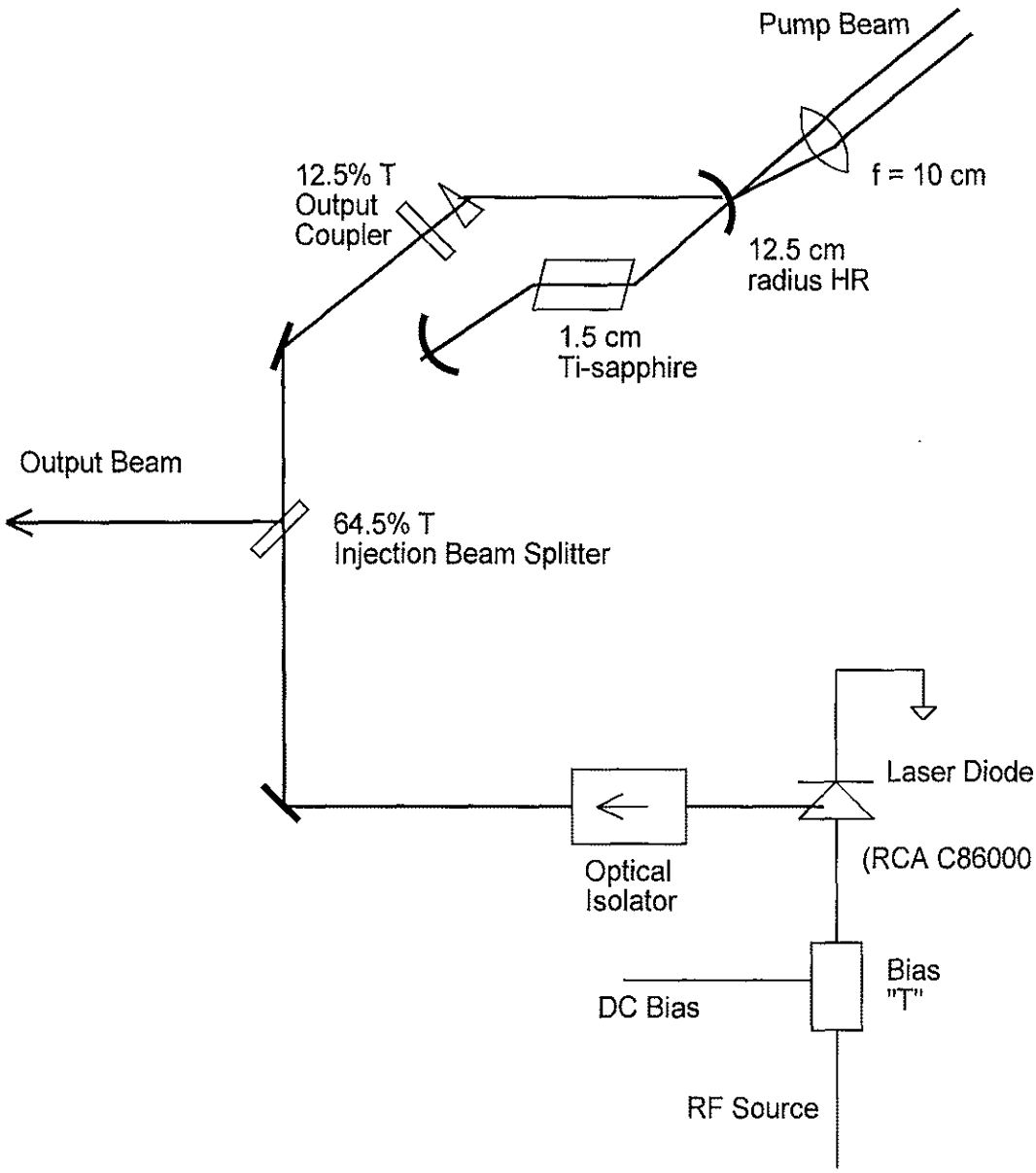


Figure 3.2 Experimental arrangement for injection seeding a Ti-sapphire laser. The pump beams are 100 ns, 532 nm pulses at 0–2 kHz [3.16].

round trip time, ~ 5 ns. The shortest pulse obtained was 19.4 ps, the same as the injected pulse.

The laser system (for this thesis) described in the next chapter is very similar to this experiment (Basu et al.). The only difference is the pump beam; instead of the doubled Q-switched Nd-YAG, the pump laser used in Basu's experiment, I used an argon-ion cw laser, and the optical frequencies of the diode laser and the modelocked Ti-sapphire laser are different.

# CHAPTER 4

# INJECTION MODELOCKED TI-SAPPHIRE LASER

The experiment was based upon the Spectra Physics 3900 Ti-sapphire laser oscillator [4.1]. It consists of a folded mirror design that was designed to operate as a free-standing laser [4.3]. The same laser has also been modified for use as an active modelocked laser and as a passive modelocked laser at other laboratories [4.4, 4.5]. Figure 4.1 shows a diagram of the CEBAF injection modelocked laser [4.2]. In our case the flat high-reflector end mirror supplied with the laser was replaced with a 2% transmissive "input" coupler, which served as an input port for the seed pulse. Both output and input coupler mirrors were wedged at $2^{\circ}$ to avoid unwanted reflections back into the laser cavity. The Ti-sapphire laser crystal (20 mm long by 5 mm dia.) was mounted on a water cooled copper heat sink and was provided by Spectra Physics. The pump laser was focused into the crystal with a 30 cm radius of curvature mirror. The absorption of the pump beam in the crystal was measured to be 80%. Included with the laser is a birefringent tuning filter that allows the free-running laser output to be adjusted between 750 nm and 900 nm [4.1]. For the purposes of this experiment it was not needed and was removed. Once it was removed, the laser operated at 852 nm. The Ti-sapphire laser emitted 700 mW through the output coupler mirror (5% transmissive) and 300 mW through the input coupler when pumped with 6 W of green light from a multi-line argon-ion laser. The lasing threshold for the Ti-sapphire laser was approximately 2 W of pump power. The cavity length was determined precisely by observing the beat signal

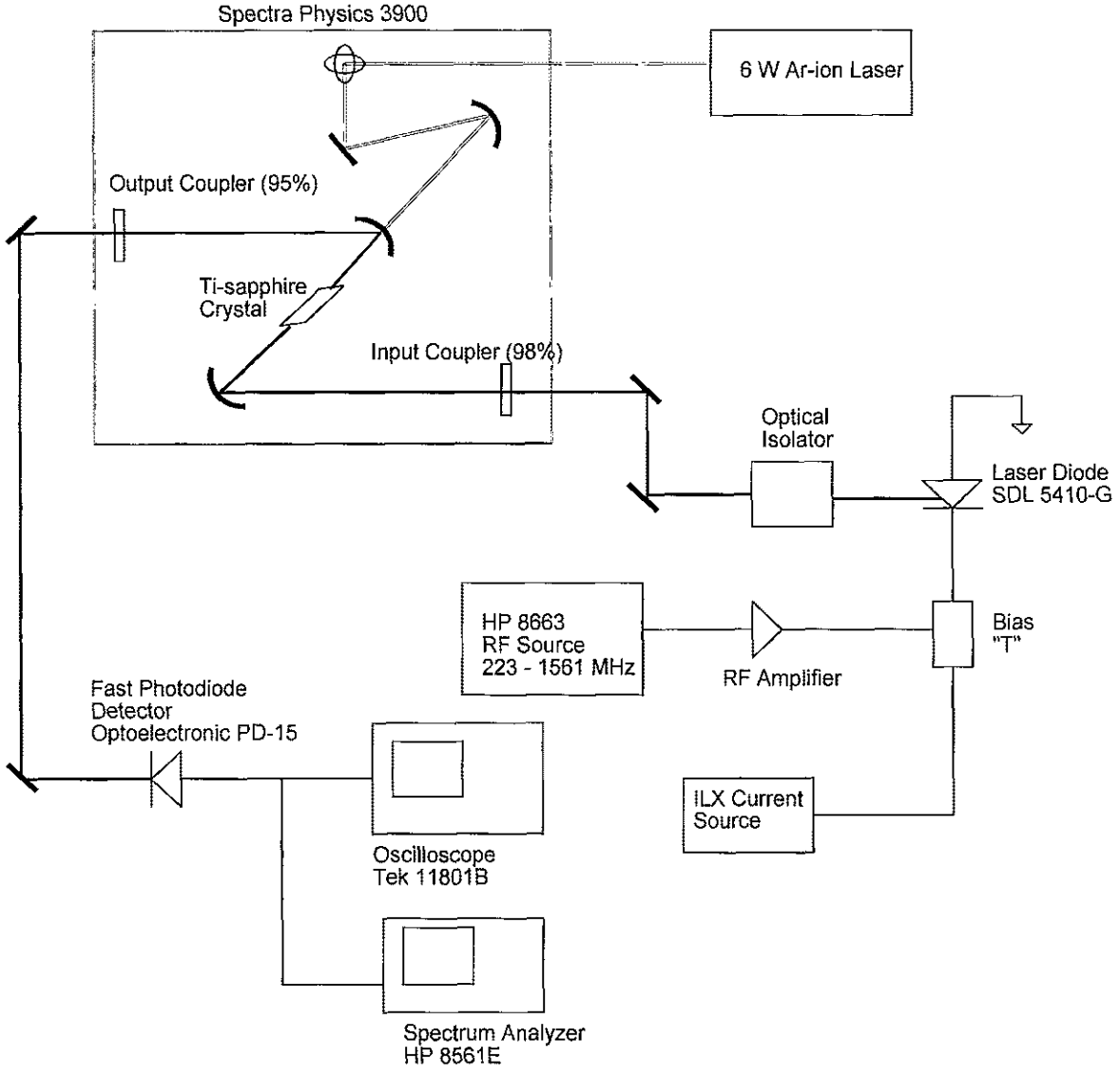


Figure 4.1 Diagram of the injection modelocked Ti-sapphire laser.

between the laser pulses using a fast photodiode (Optoelectronic Model PD-15) and an RF spectrum analyzer (HP 8561E).

The seed laser (SDL 5410-G1) was gain switched in the usual way [4.6]. The laser was biased near threshold and an RF signal (1 W) at the axial cavity frequency was applied using a biased-tee network. Originally a step-recovery diode (SRD) was used after the RF amplifier to sharpen the laser pulse, but through empirical measurements it was discovered that the gain-switched diode laser performance was not enhanced using the SRD. The pulsewidth of the diode laser was affected by the dc bias current (ILX temperature and current controller), so it was important to operate within a narrow range. Beyond this range, pulsewidths broadened and/or secondary pulses were observed (reflections from impedance changes) with the fast photodiode and sampling oscilloscope (Tektronix model 11801B with SD-32 sampling head). Biasing the laser diode near threshold does increase the chance of multi-mode operation [4.7], but the mode spacing is typically 100 GHz and has not shown itself to be a problem on the present photocathode laser system used at CEBAF. The average output power of the diode laser was approximately 5 mW. The wavelength of the diode laser was approximately 859 nm, roughly 7 nm different from the free-running Ti-sapphire laser wavelength. The gain-switched diode laser output passed through an optical isolator (approx. 40 dB of isolation) and then was directed into the Ti-sapphire laser cavity through the 2% transmissive input coupler. The polarization of the diode laser was oriented parallel to the c-axis of the Ti-sapphire crystal.

Injection modelocking was easily established once the seed laser had been spatially mode matched with the Ti-sapphire laser and the RF signal generator had been tuned to within approximately 5 kHz of the laser cavity frequency at 223 MHz. Pulsed operation was clearly evident by observing the detected output (fast photodiode) using an RF spectrum analyzer and a fast digitizing oscilloscope (Figures 4.2 and 4.3). Modelocking to higher pulse repetition rates was simply a matter of adjusting the RF signal driving the gain-switched diode to the harmonics of the laser cavity. The laser produced stable pulse repetition rates up to 1.56 GHz, the seventh harmonic of the Ti-sapphire laser cavity fundamental frequency. The average output power did not change between dc and modelocked operation; maximum average power through the output coupler was 700 mW with 6 W of pump power. The effective gain (input to output) of the injection modelocked laser was 21.5 dB. When ND filters were informally placed in front of the seed laser pulse, it was apparent that the 5 mW was considerably more than necessary to induce the Ti-sapphire laser to modelock.

It is important to note that the wavelength of the modelocked Ti-sapphire laser was 854 nm -- 2 nm different than the dc wavelength and 5 nm different from the seed laser. This suggests that the laser is truly modelocked and not acting as a multipass amplifier or injection locked laser. Injection locking requires that the slave laser lock to the optical wavelength of the injected seed laser. This is definitely not the case here. Other observations included moving the bias point on the seed laser diode tens of milliamperes to adjust for the best pulse shape out of the laser diode. This in turn would change the optical wavelength out of the laser diode. A typical gain-switched laser diode will exhibit

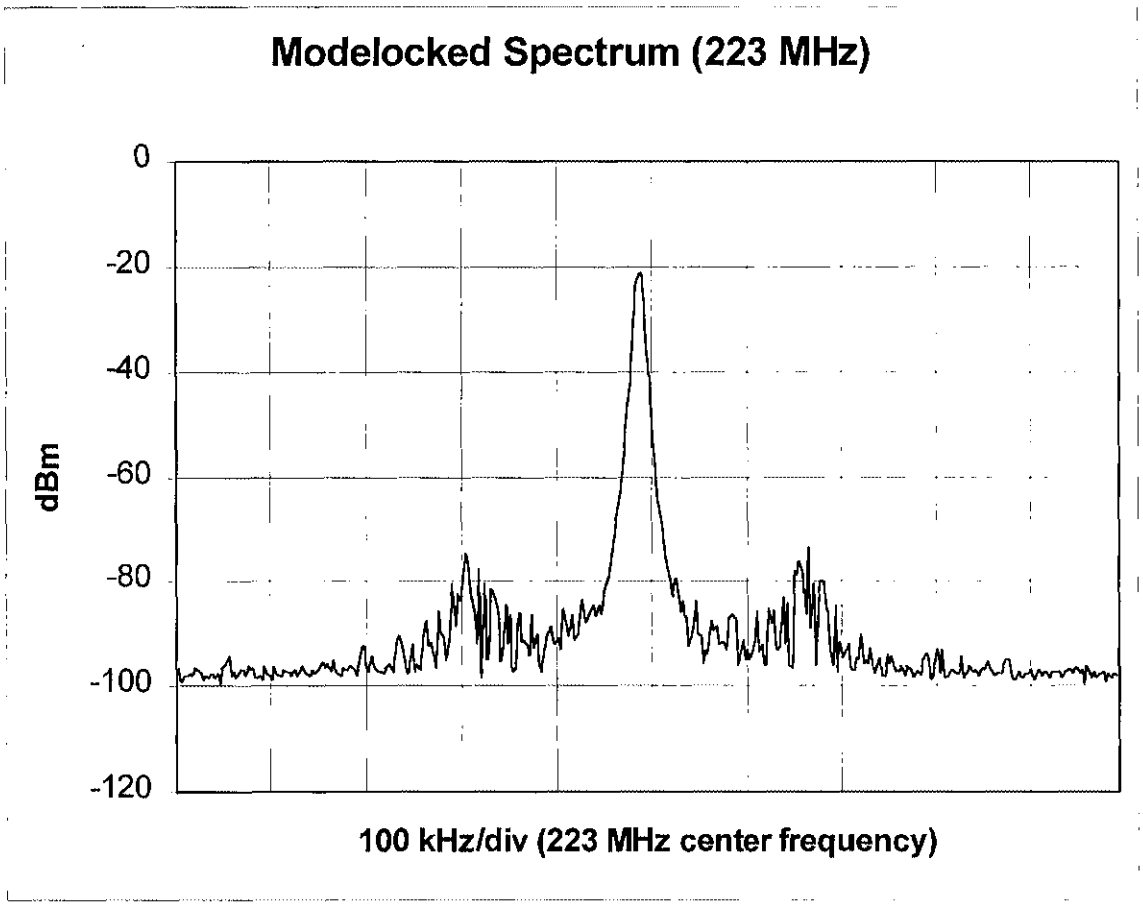


Figure 4.2 Modelocked spectrum of Ti-sapphire laser as detected using a fast photodiode. Note 0.0 dBm is defined as 1 mW.

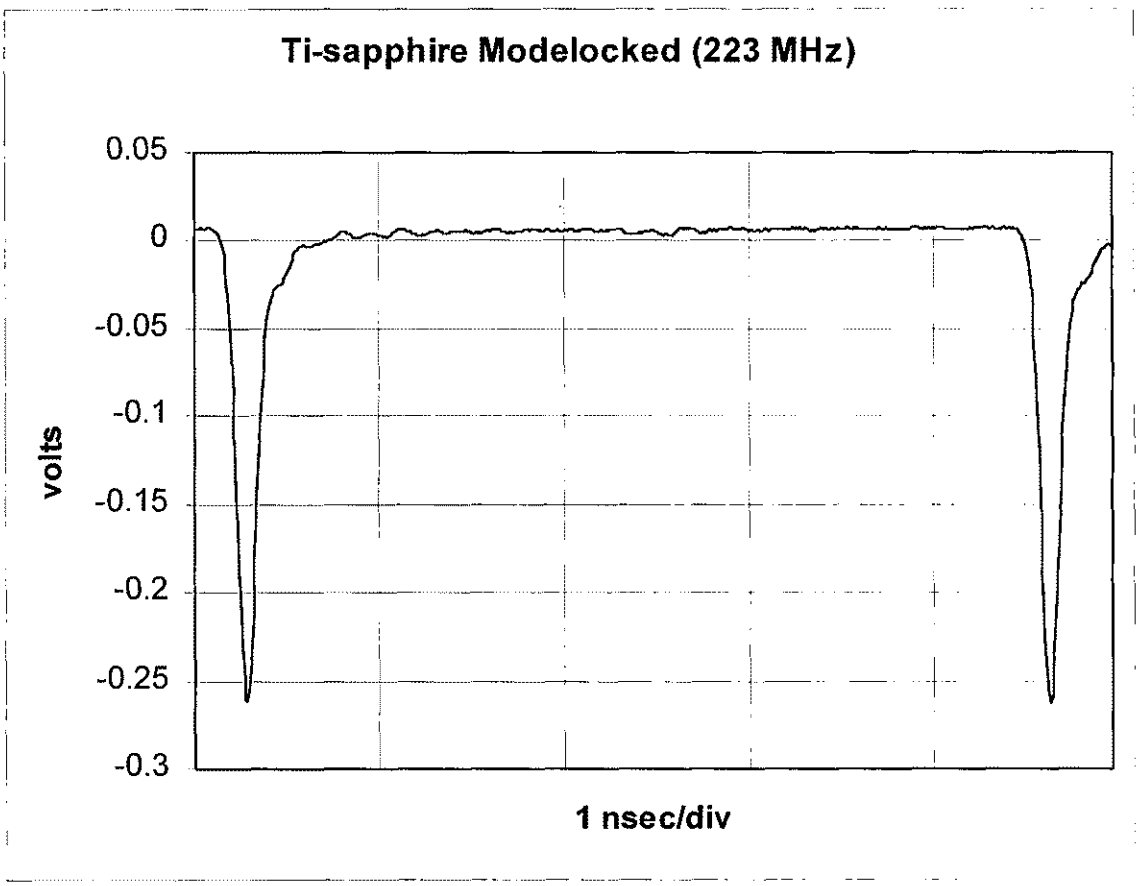


Figure 4.3 Modelocked output of Ti-sapphire laser as seen with a fast sampling oscilloscope.

3.6 GHz/mA [4.8]. Changing the laser diode's optical wavelength by these amounts did not seem to affect the output (wavelength) of the Ti-sapphire laser. If the laser were truly injection locked, changing the optical frequency by multiple GHz would drive the slave laser out of lock. In addition the laser diode temperature was held constant to 17° C by the ILX controller (for this diode the temperature coefficient for wavelength is 0.3 nm/°C [4.7]).

The laser's sensitivity to tuning across the cavity axial mode frequency decreased as you increased repetition rate. At 223 MHz the laser would stop modelocking when the source was tuned 5 kHz away from resonance. At 1561 MHz this would not happen until the source was tuned 60 kHz away from resonance. This implies that lasers cavity quality factor, "Q", is also decreasing with repetition rate, which is typical for microwave cavities. This effect will have a large implication for the laser's pulse to pulse timing jitter discussed in a later section. A possible reason for this is that these modes are not as strongly coupled to the cavity, making the injected seed laser work harder.

Finally it should be noted that the Ti-sapphire laser was operated well below saturation at a pump power of 6 W. Figure 4.4 shows a graph of the output power of the Ti-sapphire vs. the Ar-ion pump laser. It is quite linear with no sign of gain saturation. Spectra Physics specifies that this Ti-sapphire laser can handle pump lasers up to 20 W, which translates to a Ti-sapphire laser average output power of 2.5 W [4.1].

Unfortunately the laser was not very stable and would break into oscillations 10 to 30 kHz away from the carrier after a few minutes of operation. Some of this could be due to noise (power supply) measured on the Ar-ion pump beam at 36 kHz (compounded by detuning of the cavity). There were brief periods (minutes) of amplitude stable pulsed operation. Typically, however, the Ti-sapphire laser itself would drift out of alignment over time which implied that the seed laser would need to be aligned and/or the RF signal generator would have to be adjusted to account for the dimensional changes to reestablish stable output.

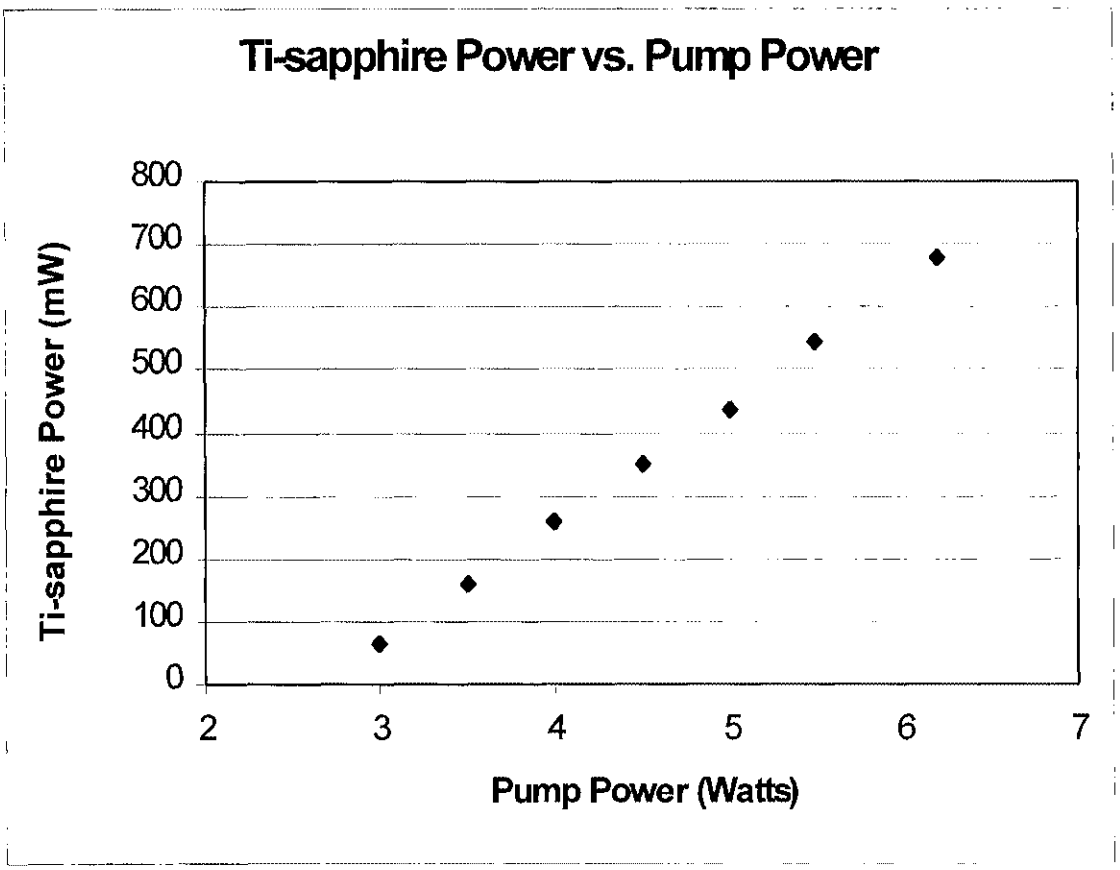


Figure 4.4 Ti-sapphire laser output power vs. Ar-ion pump power. Ti-sapphire laser is well below saturation.

# CHAPTER 5

# PHASE NOISE MEASUREMENTS

A series of measurements was performed to determine the phase stability of the injection modelocked Ti-sapphire laser. The intended application of the laser (accelerator photocathode driver) requires a high degree of phase stability. As has been stated, the frequency (repetition rate) of the laser must be a harmonic of that of the accelerating cavity, and an additional requirement is that the phase noise or timing jitter also must meet certain specifications to maintain acceptable electron beam quality. Small timing changes between laser pulses will cause the electrons coming off the photocathode not to be captured by the accelerator [5.1].

Phase noise is better known in the laser community as timing jitter [5.2]. Timing jitter is the amount of variation in time between a train of pulses. Much has been written on the subject in microwave literature, where it is an important parameter in microwave and wireless communications [5.3]. It is also important to particle accelerators, where phase noise from the RF source can affect the bunching of the electrons. The axial mode of a laser is no different than that of any other oscillator whether audio, microwave or laser. The oscillation conditions are the same and the systems can be modeled in a similar fashion. Unfortunately, injection locking to another oscillator as proposed here is not immune to phase noise degradation. An oscillator's phase noise is a product of many parameters. The noise is typically thermal noise, but line components such as 60 and 120 Hz may affect the spectrum too. The signal purity is also controlled by the bandwidth

(quality factor, "Q") of the resonating circuit used to create the oscillator. It can also degrade appreciably if it is subjected to a non-linear process such as frequency multiplication or amplifier saturation [5.4]. The injection modelocking that takes place inside the Ti-sapphire laser oscillator is a saturation process that allows the gain of one axial mode to dominate; hence the importance of the measurement.

The time between laser pulses can be represented by a sine wave with the frequency equal to the inverse period between the pulses. Theoretically one hopes the period between pulses is exact and unchanging; unfortunately there is always some finite amount of jitter associated with this period. If one Fourier transforms the time domain signal of the laser repetition rate, one gets the power spectrum and the associated noise (in the frequency domain). This noise away from the carrier frequency is called the single side-band phase noise of an oscillator and is used to characterize the quality of the oscillator. Phase noise can be measured in a variety of ways but is most typically measured using a reference oscillator that is locked to the same frequency as the oscillator under test. The signals are then compared using a diode frequency mixer or analog multiplier. Figure 5.1 shows a diagram of a phase noise measurement. The dc output of the microwave mixer is then the residual phase noise of the two oscillators (for a complete description of the mixer output, see Appendix A). Using a low frequency spectrum analyzer (dynamic signal analyzer) the single side-band phase noise can be measured. For these measurements an HP 8563B spectrum analyzer is used to measure the laser's phase noise. The spectrum analyzer uses a similar circuit as Figure 5.1 to measure the phase noise.

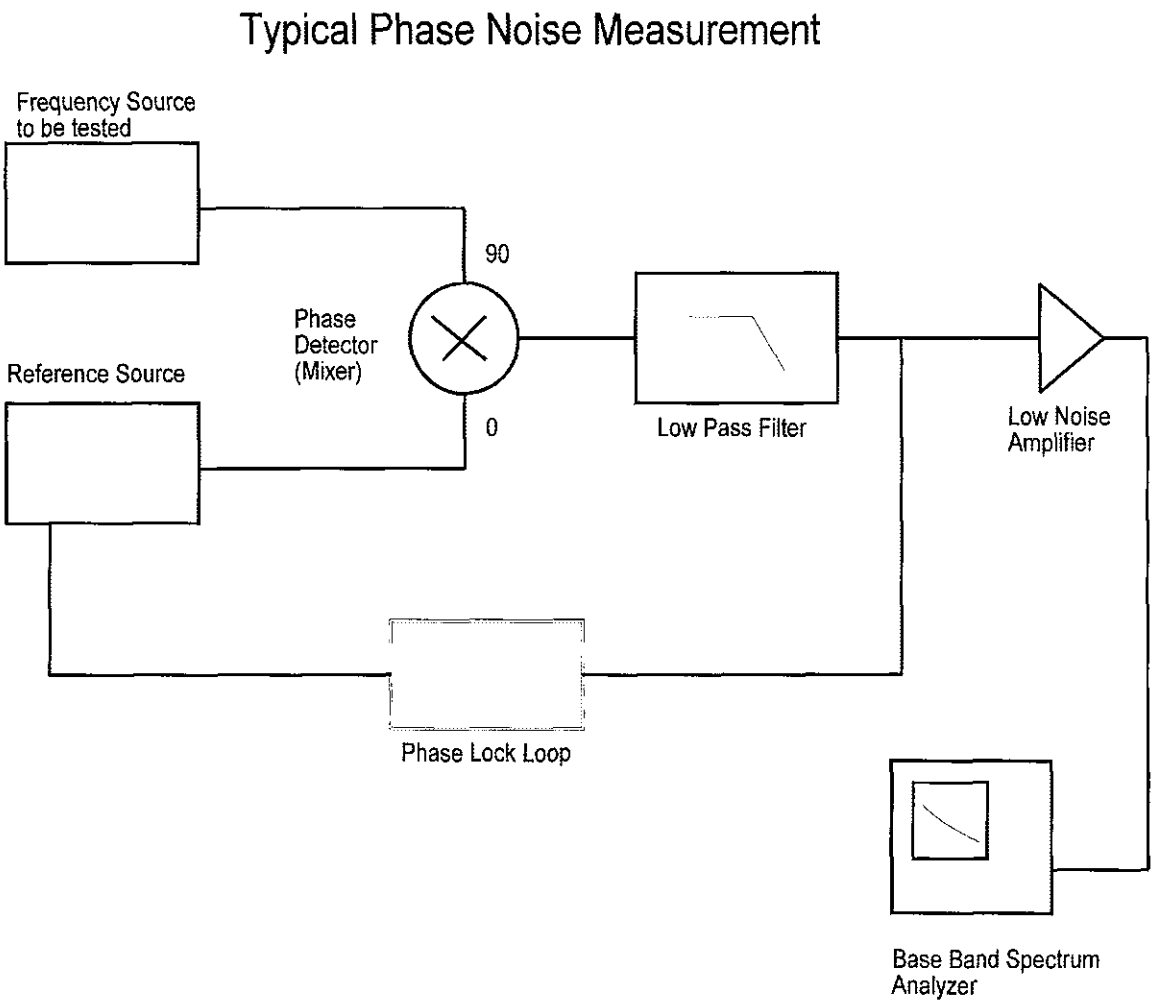


Figure 5.1 Diagram of a phase noise measurement using a mixer as a phase detector. The reference source is $V_R = \cos(\omega t)$ and the frequency source to be measured is $V_O = \cos(\omega t + \phi(t))$, where $\phi(t)$ is the time dependent phase noise or jitter.

A fundamental definition of phase instability or phase noise is the one-sided spectral density of phase fluctuations on a per-Hz basis. Spectral density describes the energy distribution as a continuous function which can be described in units of energy within the specified bandwidth [5.3].

$$S_{\Delta\phi}(f) = \frac{\Delta\phi^2{}_{rms}}{\text{Bandwidth}} \quad \text{rad}^2/\text{Hz} \qquad (5.1)$$

In most oscillator cases since the total phase deviations are small ( $\Delta\phi_{pk} << 1$ radian), another useful relationship for noise energy is L(f), which is directly related to $S_{\Delta\phi}(f)$ by

$$L(f) = \frac{1}{2} S_{\Delta\phi}(f) \qquad (5.2)$$

L(f) is usually presented logarithmically as a spectral density plot of the phase modulation sidebands in the frequency domain and is expressed in dB relative to the carried per Hz (dBc/Hz). An extremely useful number derived form the spectral density is the integrated phase noise [5.5]. The integrated phase noise is a measure of the phase noise contribution (rms radians, rms degrees) over a designated range of Fourier frequencies. The integration process is a process of summation on the spectral density within the measurement bandwidth. Since the spectral density is usually normalized to a bandwidth (Hz) it must be unnormalized. Therefore

$$S_{\Delta\phi}(f) = 2\left[10^{D}\right] \qquad D = \left[L(f) + 10\log(BW)\right]/10 \qquad (5.3)$$

where BW is the bandwidth of the measurement (typically 1 Hz), and L(f) is the log spectral density plot. The dimensions are now in radians squared. The integrated rms phase noise in radians is

$$S_{rms}(f_1 \rightarrow f_n) = \sqrt{\sum S_{\Delta\phi}(f_1) + S_{\Delta\phi}(f_2) + .....S_{\Delta\phi}(f_n)} \qquad (5.4)$$

Using the integrated phase noise, quick comparisons of oscillators can be made. To convert from rms phase noise to timing jitter one simply equates the carrier frequency ($f_c$) to $\Delta\phi_{rms}$ such that

$$\Delta\tau_{rms} = \frac{S_{rms}}{2\pi f_c} \qquad (5.5)$$

The phase noise plot displayed by the HP 8563B is measured in dBc/Hz (y) vs. frequency (x), typically 10 Hz to 1 MHz. The spectrum analyzer also performs the summation for the rms phase noise. The number of Fourier frequencies (points in the summation) is 600 and the result is given in both radians and degrees

Figure 5.2 shows a plot of the source oscillator's (HP 8663) phase noise. For this particular spectral density plot the source oscillator's rms phase noise is approximately $0.1^\circ$ or 1.75 mrads (@ 223 MHz). The timing jitter for this oscillator is then 1.2 ps. Figure 5.2 also shows the output from the pulsed seed laser. Comparing the seed laser's phase noise to that of the source, the phase noise is almost identical and within the

statistical limits of the spectrum analyzer. It should be noted that the signal source for the test, the HP 8663, is better than the signal source in the spectrum analyzer, so in effect we are measuring the phase noise of the HP spectrum analyzer in these two measurements. Given the baseline we can use these two measurements to compare to the Ti-sapphire output.

The upper plot of Figure 5.2 shows the phase noise spectrum of the Ti-sapphire laser at the axial mode frequency of 223 MHz. Comparing this to the signal source, one notices an overall increase in noise in the plot of about 10 to 20 dBc depending on the frequency. Possible reasons for this are: an unstabilized laser cavity, pump beam power supply and nonlinear processes in the gain medium. Still the integrated rms phase noise is only twice that of the signal sources, $0.2^{o}$ vs. $0.1^{o}$, respectively. This compares favorably with the Jefferson Lab IRFEL modelocked drive laser (Nd:YLF) that has a reported rms phase noise on the order of $0.3^{o}$ [5.6].

Figure 5.3 shows the integrated rms phase noise for selected axial modes (from 223 MHz to 1561 MHz). The phase noise gradually increases with the axial mode frequency. This is due to the fact that the loaded Q of the axial mode decreases with frequency effectively increasing the noise bandwidth. Think of the cavity as a filter! As mentioned previously the stability of the laser system and the lengthy time (3 minutes) to make a phase noise measurement meant that it was difficult to get a clean measurement. The

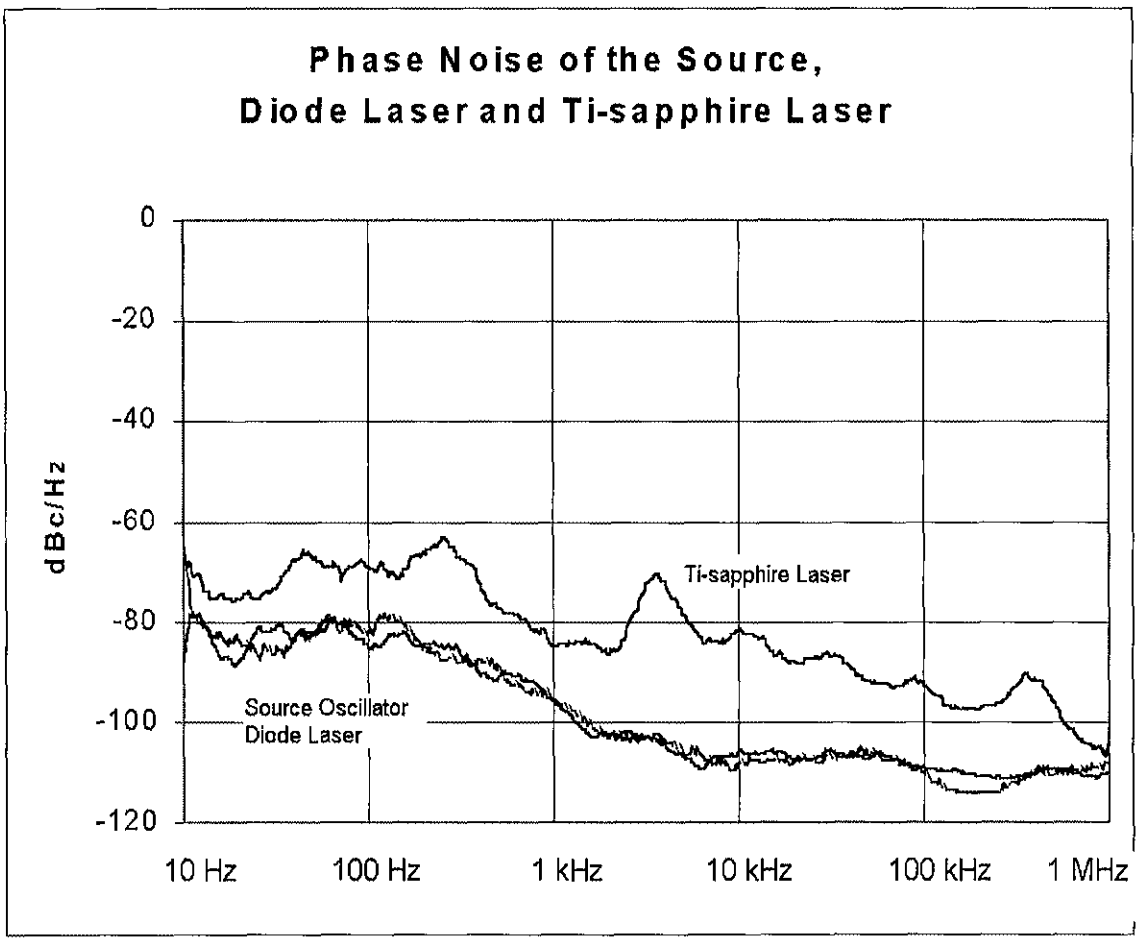


Figure 5.2 Phase noise measurements of the source oscillator, the output of the diode laser and the output of the Ti-sapphire laser. The phase noise of the source and the diode laser are statistically identical.

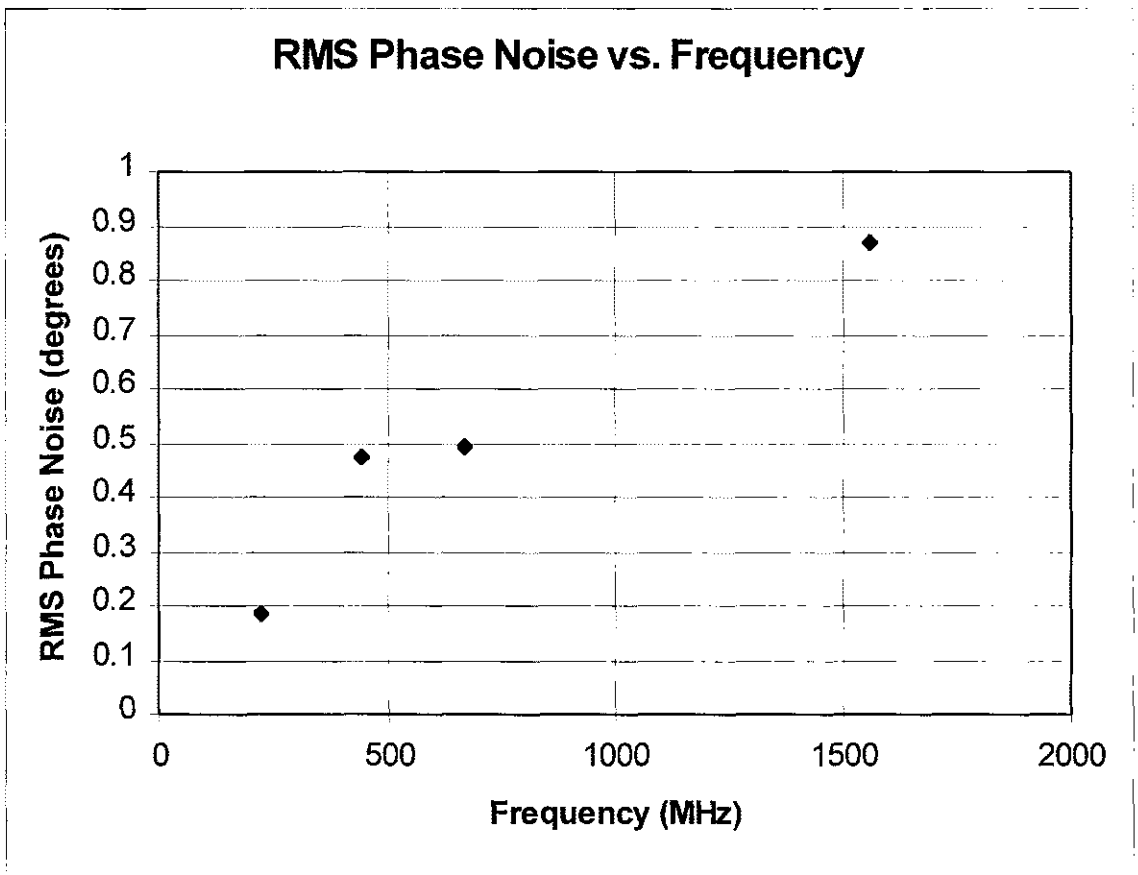


Figure 5.3 Integrated rms phase noise of the fundamental (223 MHz) and higher axial modes of the Ti-sapphire laser.

phase noise reported is the best that the system was able to do with only injection locking and no cavity stabilization.

In addition to the phase noise measurements, a transfer function measurement was made to determine the laser cavity's Q. The Q of the resonant circuit used for the oscillator dominates the phase noise term [5.7]. Since we are using an injected oscillator the output is subject to its own phase and therefore its own Q plays a major role in the phase noise. The laser can be modeled as a closed loop steady state system with the cavity as the resonating circuit and the gain medium the Ti-sapphire crystal [5.7]. If this is done then the predicted system phase noise of an oscillator is

$$S_{\Delta\phi}(f) = \frac{2FkT}{Ps}\left[1+\left(\frac{f_o}{2Qf_m}\right)^2\right] \qquad (5.6)$$

where F is the noise figure of the amplifier, k is Boltzmann's constant, T is temperature in Kelvin, Ps is the oscillator output power, $f_o$ is the carrier frequency, and $f_m$ is the frequency offset from the carrier. The important aspect of equation 5.6 is the dependence on Q. The effect is great; the phase noise of an oscillator with a Q of 10,000 is 20 dB higher than an oscillator with a Q of 100,000!

To determine the Q of the axial mode resonance an empirical measurement was performed. Figure 5.4 shows the measurement technique, which is basically a measurement of the gain bandwidth of the axial mode. The laser was injection seeded

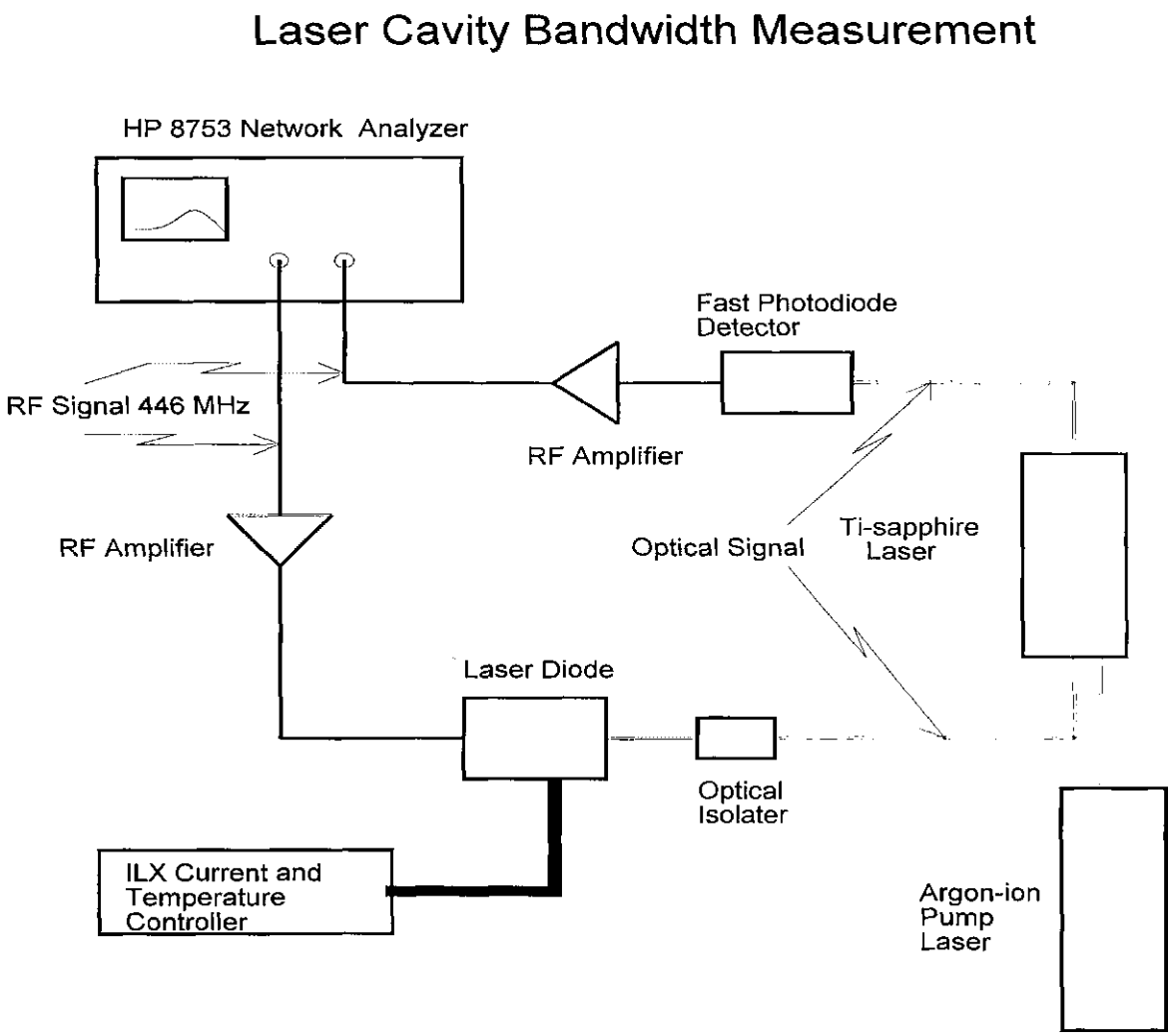


Figure 5.4 Diagram of the Ti-sapphire laser cavity bandwidth measurement. Measurement was performed at the 2nd cavity harmonic because a narrow band SRD was used to shorten the pulsewidth into the laser diode.

with the diode laser at a repetition rate of 450 MHz. A fast diode detector was then used to detect the laser pulses after the Ti-sapphire laser. Instead of using an RF signal source an RF Vector Network Analyzer (VNA, HP8753C) was substituted. The VNA has the ability of measuring the loss/gain through a network over a desired frequency range (transmission measurement). Using the transmission measurement we can then measure the cavity's loaded quality factor ($Q_L$) and the 3 dB bandwidth. Figure 5.5 shows a plot of this measurement. The loaded Q was measured to be approximately 85,000 with a 3 dB bandwidth of approximately 5 kHz. This compares favorably with a good quartz crystal and implies that with active feedback (cavity length control) the system could be made to have very low phase noise.

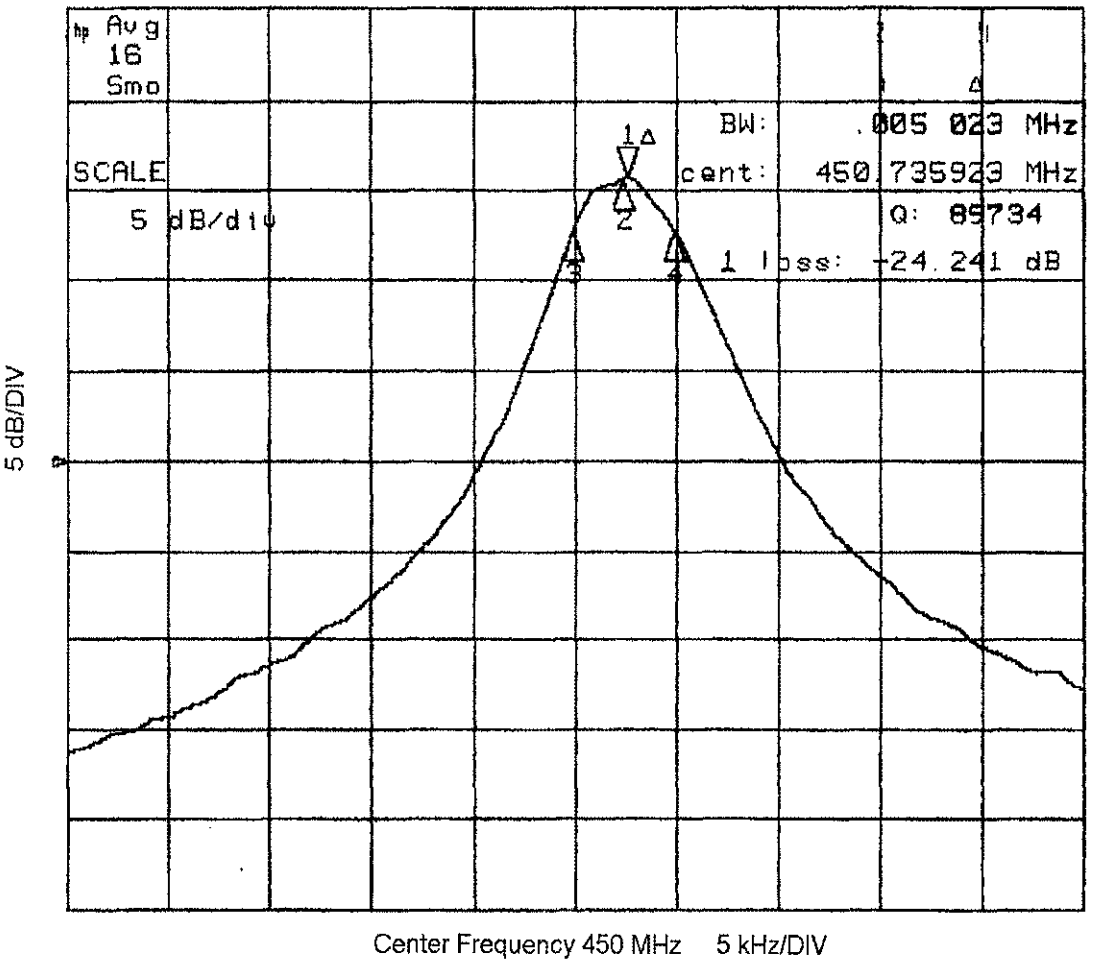


Figure 5.5 Swept frequency transmission measurement of the Ti-sapphire laser cavity. The cavity Q is 85374. The cavity's 3 dB bandwidth is approximately 5 kHz.

# CHAPTER 6

# PULSEWIDTH MEASUREMENTS

The laser pulsewidth is an important factor in designing a photocathode, because of the process in which electrons are emitted from the photocathode [6.1]. Typically a photocathode is illuminated for 30 to 60 ps and an electron pulse of similar length is emitted. The electron current is a function of the quantum efficiency of the photocathode. The electron optics is designed to accommodate a certain electron pulsewidth and current. If the pulsewidth is too short the electrons can undergo space charge effects that increases the effective bunchlength. If the laser pulsewidth is too long the electron optics can't capture all of the electrons, and they are wasted. Given the relative short lifetime of photocathodes it is important that the laser pulse is such that all the electrons are used. Therefore the ability of the Ti-sapphire laser to effectively transmit the seed diode's pulsewidth and shape with no degradation is important for the application.

Ti-sapphire lasers as mentioned earlier are used extensively in short pulse research [6.2, 6.3, 6.4]. Their broad linewidth allow for extremely short pulsewidths. Commercial Ti-sapphire lasers (with modelocking) similar to the one that we are using have been modified to deliver repeatable pulsewidths of less than 1 ps [6.4]. Therefore there was some concern this injection modelocked system would undergo some pulsewidth compression.

The pulsewidth measurement consisted of using a commercial second harmonic autocorrelator. A variety of pulsewidths were measured at different pulse repetition rates and varying the laser pump power. A concern was how the pulsewidth would change as the pulse repetition rate (for electron bunching reasons) was increased and as the pump power was changed.

The most popular method used to measure short pulses is a correlation method that compares two similar signals together while sweeping one of them, in time, against the other (note that the phase noise measurement is also a correlation measurement but at microwave frequencies). The correlation method typically used is the noncollinear (background free) second harmonic generation (SHG) technique [6.5]. In this measurement an autocorrelation is made by splitting the signal into two identical signals and sweeping one across the other, a form of convolution. The normalized second order autocorrelation function is given by [6.5]

$$R^2(\tau) = \frac{\langle I(t)I(t+\tau)\rangle}{\langle I^2(t)\rangle} \qquad (6.1)$$

where

$$\langle f(t)\rangle = \int_{-\infty}^{\infty} f(t)dt, \qquad (6.2)$$

and I(t) is the instantaneous intensity of the signal. A disadvantage of this method is that the correlation function gives no information about pulse shape. In the case of the SHG technique the output is always symmetric no matter what the shape of the measured pulse

I(t). Pulse shape can be obtained from higher order correlation functions if other methods are not available. In this thesis it was assumed to be Gaussian.

Figure 6.1 shows a diagram of the "Femtochrome model FR-103XL" autocorrelator used for the measurement [6.6]. The laser pulse is sent into the interferometer where one leg has an adjustable delay. The autocorrelator uses a pair of rotating mirrors to continuously sweep the delay of one of the pulses. The total scan (in ps) range of the autocorrelator is then a function of the rotating mirror diameter "d".

$$T = \frac{\sqrt{2}}{c} d \qquad (6.3)$$

For this autocorrelator the mirror diameter is 2.54 cm, which gives a span of 120 ps. SHG is produced when the two pulses are phase matched at the SHG crystal ($LiIO_3$). The SHG signal is in a direction bisecting the two beam paths and is only present when the pulses overlap. The SHG signal is focused onto a photomultiplier tube (PMT). By measuring the integrated SHG intensity versus the relative delay between the two pulses a direct measurement of $R^2(t)$ is made. When the PMT signal is placed onto an oscilloscope that is synchronized to the rotation frequency of the mirrors, a continuous display of the autocorrelation function is observed on the oscilloscope. A simple form factor (32ps/ms), that is a function of the distance between the rotating mirrors and the rotation frequency, is used to calculate the pulsewidth. As an example, if the scope shows an FWHM trace of 1.0 ms (assuming a Gaussian pulse shape, multiply by 0.707) the pulsewidth is then 22.6 ps. The autocorrelator traces for the diode seed laser (35.5 ps FWHM) and the injection

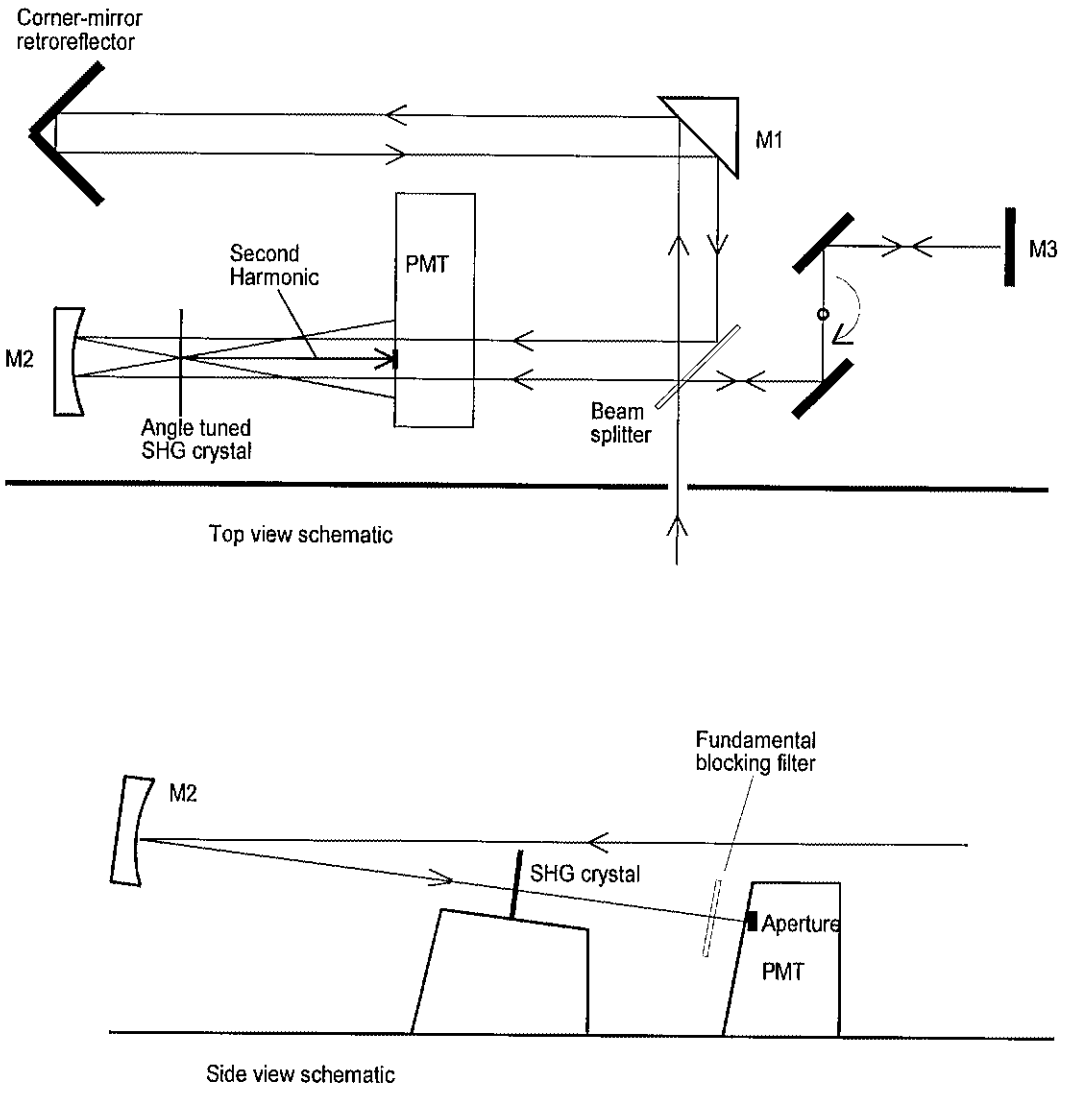


Figure 6.1 Top view schematic of the FR-10XL background free autocorrelator (top), and the side view (bottom) [6.6].

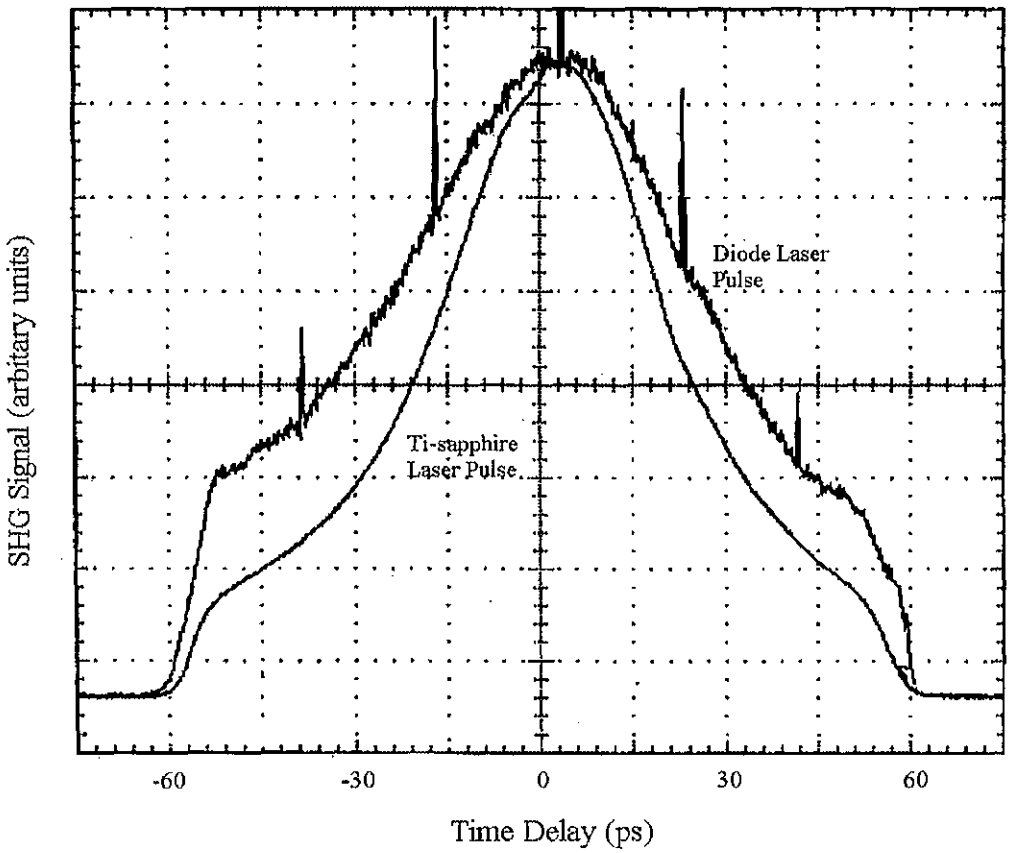


Figure 6.2 Autocorrelator trace of the diode seed laser and the injection modelocked Ti-sapphire laser. To determine actual pulsewidth, the autocorrelation pulsewidth was multiplied by 0.707 to account for a Gaussian pulse shape. Note that the clipped edges are not indicative of actual pulse shapes. The maximum temporal resolution of the autocorrelator is approximately 120 ps.

modelocked Ti-sapphire laser (27.8 ps FWHM) at a pulse repetition rate of 223 MHz are shown in Figure 6.2. The spikes on the seed laser pulse are typical for diode lasers. The spikes are separated by the round trip time of the diode laser cavity and are indicative of the random phase relationship that exists between the different longitudinal modes excited during the gain-switching process [6.1].

The pulsewidths out of the Ti-sapphire laser varied depending on the pump power. Figure 6.3 shows a graph of the pulsewidth (FWHM) vs. the Ti-sapphire power. At the lower pump power (3 W) the pulsewidth was a factor of two narrower than at the highest pump power (6 W). This can be possibly be due to the fact that at the lower pump power levels the Ti-sapphire laser is just beginning to lase, which can narrow the pulse due to gain saturation effects.

It was verified that the pulsewidth decreases as the repetition rate increases. Figure 6.4 is a graph of pulsewidth vs. axial mode frequency. The pulsewidth of a laser is a function of the sidebands of the fundamental pulse [6.7]. The more sidebands sustainable within the linewidth, the sharper the pulse. The Ti-sapphire laser has a linewidth of approximately 40 GHz [6.8]. At 223 MHz this corresponds to approximately 179 sidebands of the axial mode frequency, as opposed to 1115 MHz, which can only support 36.

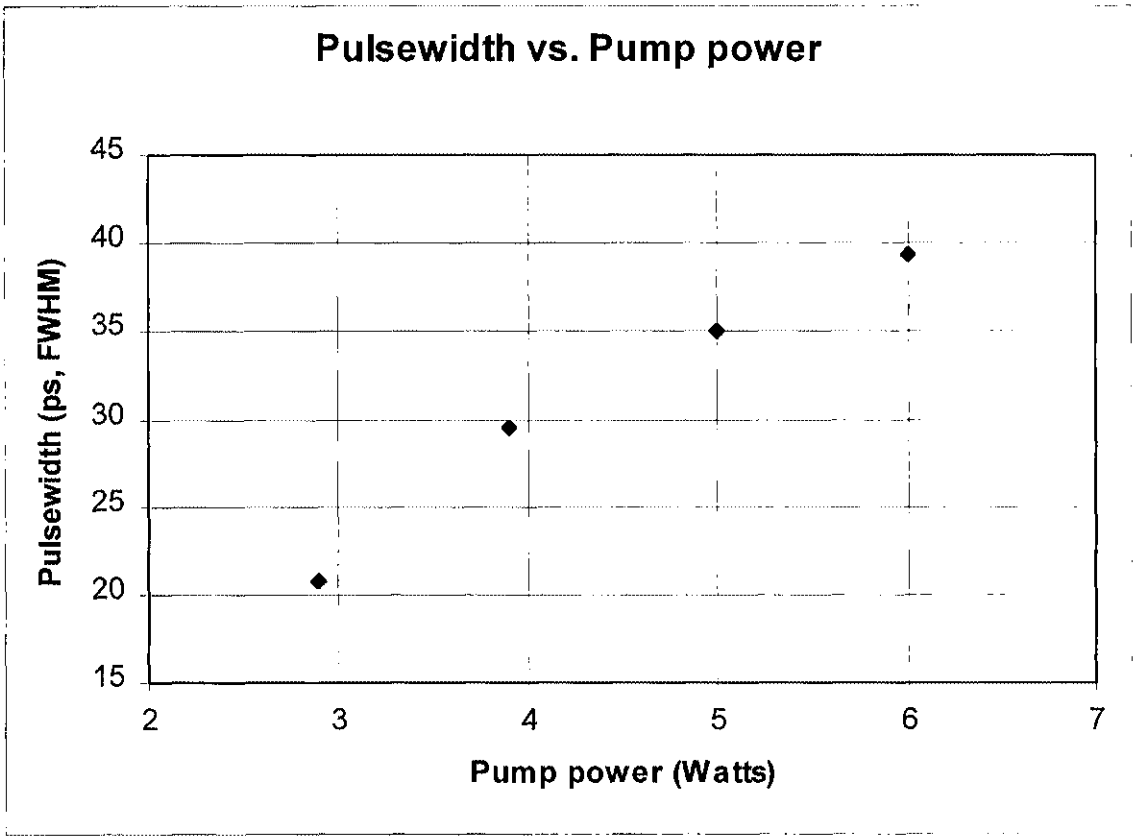


Figure 6.3 Graph of Ti-sapphire pulsewidth vs. pump power. The pulsewidth decreases at the lower pump powers due to gain saturation effects in the Ti-sapphire crystal.

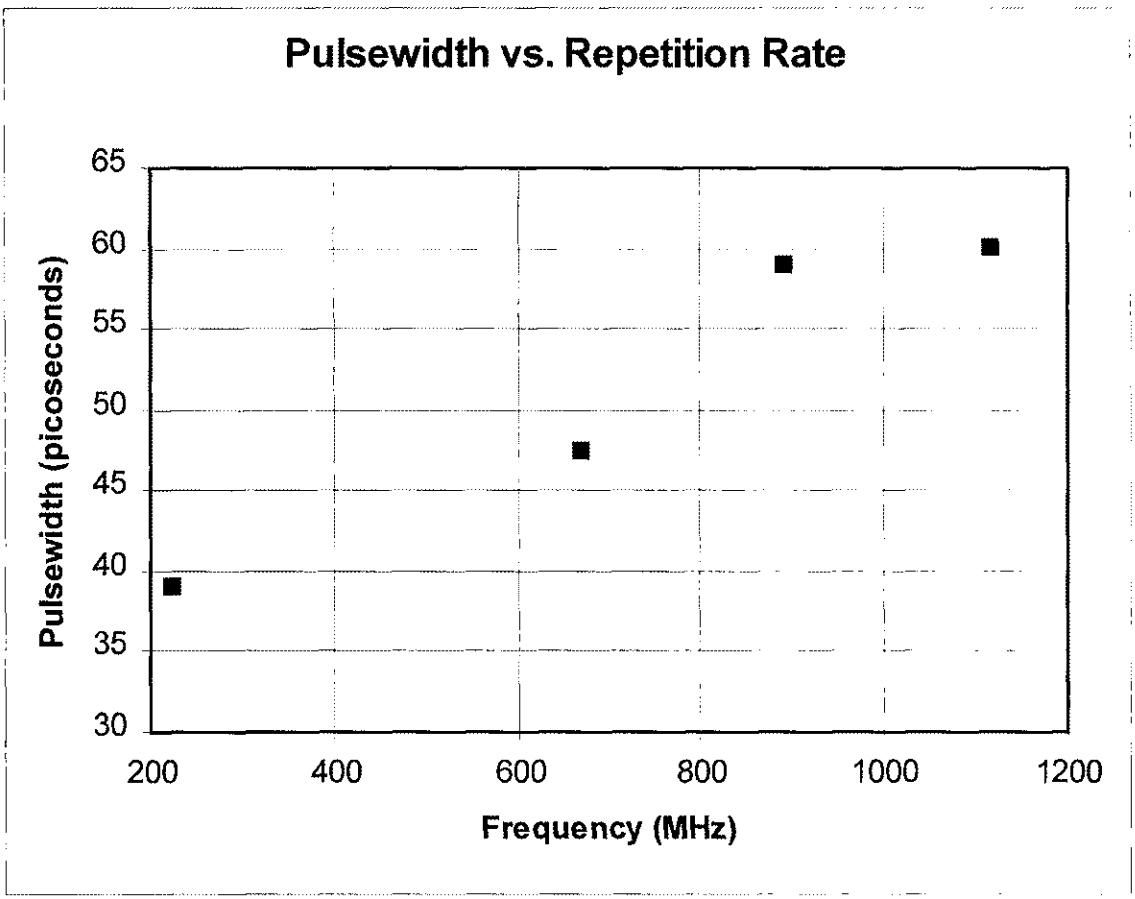


Figure 6.4 Graph of the pulsewidth versus repetition rate of the injection modelocked Ti-sapphire laser. The pulsewidth increases with frequency due to fewer active modes being made available at the higher repetition rates.

# CHAPTER 7

# CONCLUSION

I have demonstrated the ability to injection modelock a Ti-sapphire laser. All indications point to a modelocked pulsetrain emanating from the Ti-sapphire laser. Specifically the Ti-sapphire laser had a different optical frequency than the diode seed laser. Average output powers approached 1 W, which is higher than the diode/ amplifier laser system presently used. Output laser pulsewidths ranged from 21 to 39 ps (FWHM) and could provide a manageable electron beam at Jefferson Lab that is not dominated by severe space charge effects. The pulse to pulse timing jitter (phase noise) compared favorably to present laser systems and would not hinder the laser's use in an electron accelerator. An important aspect demonstrated in the investigation is the ability to modelock the laser at harmonic frequencies above the lowest axial mode frequency. This allows one to design a cavity with practical dimensions but still deliver output pulses at repetition rates above 1 GHz. Stability issues concerning cavity drift were not addressed, but could possibly be overcome by applying active feedback to the laser cavity. The results presented here provide "proof of principle" that injection modelocking a Ti-sapphire laser using a gain switched diode laser is a promising method to obtain high power, pulsed laser light with GHz pulse repetition rates.

# REFERENCES

*Chapter 1*


1.1 P. F. Moulton, "Spectroscopic and laser characteristics of Ti:$Al_2O_3$," J. Opt. Soc. Am. B, Vol. 3, No. 1, Jan. 1986, pp. 125 – 133.

1.2 A. Sanchez, R. E. Fahey, A. J. Strauss, and R. L. Aggarwal, "Room-temperature continuous-wave operation of a Ti:$Al_2O_3$ laser," Opt. Lett., Vol. 11, No. 6, June 1986, pp. 363 – 364.

1.3 R. Roy, P. A. Schulz and A. Walther, "Acousto-optic modulator as an electronically selectable unidirectional device in a ring laser," Opt. Lett., Vol. 12, No. 9, Sept. 1987, pp. 672 – 674.

1.4 A. J. Alfrey, "Modeling of Longitudinally Pumped CW Ti:Sapphire Laser Oscillators", IEEE J. Quantum Electron., Vol. 25, pp. 760 – 766, No. 4, April 1989.

1.5 J. Frisch, R. Alley, M. Browne, M. Woods, Proceedings of the 1993 Particle Accelerator Conference, Washington D. C., May 1993, pp. 3047 – 3049.

1.6 C. Hovater and M. Poelker, "An Injection Modelocked Ti-Sapphire Laser for Synchronous Photoinjection", Proceedings of the 1997 Particle Accelerator Conference, Vancouver B. C., May 1997, to be published.

1.7 P. Hartmann, J. Bermuth, J. Hoffmann, S. Kobis; Nucl. Instr. and Meth. A 379, (1996), 15.

1.8 B. M. Dunham, "Investigations of the Physical Properties of Photoemission Electron Sources for Accelerator Applications", Ph.D. Dissertation (physics), 1993, University of Illinois.

1.9 J. E. Clendenin, "Polarized Electron Sources", Proceedings of the 1995 Particle Accelerator Conference, Dallas Texas, May 1995.

1.10 D.T. Pierce, R. J. Celotta, G.-C. Wang, W. N. Unertl, A. Galejs, C. E. Kuyatt, and S. R. Mielczarek, "GaAs spin polarized electron source"; Rev. Sci. Instrum., 51(4), Apr., 1980.

1.11 M. Poelker, "High power gain-switched diode laser master oscillator and amplifier", Appl. Phys. Lett. 67(19), 6 Nov. 1995.

1.12 S. Benson and M. Shinn, "Development of an Accelerator-Ready Photocathode Drive Laser at CEBAF", Proceedings of the 1995 Particle Accelerator Conference, Dallas Texas, May 1995.

1.13 G.D. Gates et al., "The Bates Polarized Electron Source", Nucl. Instr. and Meth. A 278, (1989), 293-317.

1.14 A. Fry, M. Fitch, A. Melissinos, N. Bigelow, B. Taylor, F. Nezrick, " Laser System for the TTF Photoinjector at Fermilab", Proceedings of the 1997 Particle Accelerator Conference, Vancouver B. C., May 1997, to be published.

1.15 R. Sheffield, " High-Brightness Electron Injectors: A Review", Proceedings of the 1989 Particle Accelerator Conference, Chicago Ill., March 1989, pp. 1098 – 1101.

1.16 R. Alley et al., "The Stanford linear accelerator polarized electron source", SLAC-PUB-95-6489.

*Chapter 2*

2.1 P. Hartmann, J. Bermuth, J. Hoffmann, S. Kobis; Nucl. Instr. and Meth. A 379, (1996), 15.

2.2 G. Cerullo, S. De Silvestri, and V. Magni, " Self-starting Kerr-lens mode locking of a Ti:sapphire laser", Opt. Lett., Vol. 19, No. 14, July 15, 1994, pp. 1040 –1042.

2.3 J. A. Squier, "Development of High Average Power Femtosecond Chirped Pules Amplification Sources Using Chromium, Neodymium, and Titanium doped Materials", Ph.D. Dissertation, 1992 University of Rochester, Rochester NY. pp. 41 – 44.

2.4 H. Haus, J. Fujimoto, E. Ippen, " Analytic Theory of Additive Pulse and Kerr Lens Mode Locking", IEEE J. Quant. Elec. , Vol 28, No. 10, Oct. 28, 1992, pp. 2086.

2.5 S. Benson and M. Shinn, "Development of an Accelerator-Ready Photocathode Drive Laser at CEBAF", Proceedings of the 1995 Particle Accelerator Conference, Dallas Texas, May 1995.

2.6 A. E. Siegman, "LASERS", University Science Books, 1986; Ch 27, pp. 1056.

2.7 A. Fry, M. Fitch, A. Melissinos, N. Bigelow, B. Taylor, F. Nezrick, " Laser System for the TTF Photoinjector at Fermilab", Proceedings of the 1997 Particle Accelerator Conference, Vancouver B. C., May 1997, to be published.

2.8 R. Alley et al., "The Stanford linear accelerator polarized electron source", SLAC-PUB-95-6489.

2.9 J. Frisch, R. Alley, M. Browne, M. Woods, Proceedings of the 1993 Particle Accelerator Conference, Washington D. C., May 1993, pp. 3047 – 3049.

2.10 M. Poelker, "High power gain-switched diode laser master oscillator and amplifier", Appl. Phys. Lett. 67(19), 6 Nov. 1995.

2.11 M. Ciarrocca, H. Avramopoulos, C. Papanicolas, "A modelocked semiconductor laser for a polarized electron source", Nucl. Instr. Meth., A 385 (1997) 381 – 384.

2.12 P. O'Shea, "Jitter Sensitivity in Photoinjectors," Proceedings of the 1995 Particle Accelerator Conference, Dallas Texas, May 1995.

*Chapter 3*

3.1 A. J. DeMaria, D. A. Stetser, W. H. Glenn, "Ultrashort Light Pulses," Science, vol. 156, no. 3782, June 1967, pp. 1557 – 156.

3.2 A. Fry, M. Fitch, A. Melissinos, N. Bigelow, B. Taylor, F. Nezrick, " Laser System for the TTF Photoinjector at Fermilab", Proceedings of the 1997 Particle Accelerator Conference, Vancouver B. C., May 1997, to be published.

3.3 S. Benson and M. Shinn, "Development of an Accelerator-Ready Photocathode Drive Laser at CEBAF", Proceedings of the 1995 Particle Accelerator Conference, Dallas Texas, May 1995.

3.4 R. Adler, "A study of Locking Phenomena in Oscillators," Proc. IEEE, vol. 62, no. 10, Oct. 1973, pp. 1380 – 1385.

3.5 A. E. Siegman, "Lasers," University Science Books, Mill Valley, CA, 1986, Ch 24, 27 and 29.

3.6 C. J. Buczek, R. J. Freiberg, and M. L. Skolnick, "Laser Injection Locking," Proc. IEEE, vol. 61, no. 10, Oct. 1973, pp. 1411 – 1431.

3.7 J. Squire, F. Salin and G. Mourou, " 100-fs pulse generation and amplification in Ti:$Al_2O_3$, Opt. Lett., Vol. 16, No. 5, March 1, 1991, pp. 324 – 326.

3.8 P. Georges, F. Estable, F. Salin, J. P. Poizat, P. Grangier, and A. Brun, "High – efficiency multipass Ti:sapphire amplifier for continuous-wave single mode laser," Opt. Lett., Vol. 16, No. 3, Feb. 1, 1991, pp. 144 – 146.

3.9 J-L Lachambre, P. Lavigne, G. Otis and M. Noel, "Injection Locking and Mode Selection in TEA-CO2 Laser Oscillators," IEEE J. Quant. Electron., vol QE-12, pp. 756 –764.

3.10 Y. K. Park, "Frequency and Mode Control of Q-Switched Neodymium:YAG Lasers," Ph.D. Dissertation, Stanford University, Stanford CA., Oct. 1980, pp. 4 – 56.

3.11 Y. K. Park, G. Giuliani, and R. L. Byer, "Single Axial Mode Operation of a Q-Switched Nd:YAG Oscillator by injection Seeding," IEEE J. Quant. Electron., vol. QE-20, no. 2, Feb. 1984, pp. 117 – 125.

3.12 C. H. Bair, P. Brockman, R. V. Hess, and E. A. Modlin, "Demonstration of Frequency Control and CW Laser Diode Injection Control of a Titanium-Doped Sapphire Ring Laser with No Internal Optical Elements," IEEE J. Quant. Electron., vol. QE-24, no. 6, June 1988, pp. 1045 - 1048.

3.13 J. C. Barnes, N. P. Barnes, L. G. Wang, and W. Edwards, "Injection Seeding II: Ti:$Al_2O_3$ Experiments," IEEE J. Quant. Electron., vol. QE-29, no. 10, Oct. 1993, pp. 2684 – 2692.

3.14 E. I. Moses, J. J. Turner, and C. L. Tang, "Mode locking of laser oscillators by injection locking," Appl. Phys. Lett., vol. 28, no. 5, March 1976, pp. 258 – 260.

3.15 S. Basu, "A High Peak and High Average Power Nd:GLASS Moving Slab Laser for Soft X-Ray Generation," Ph.D. Dissertation, Stanford University, Stanford CA. 1988, pp. 106 – 138.

3.16 S. Basu, P. May, and J-M Halbout, "64-dB amplification of 19 psec laser-diode pulses in a Ti-sapphire laser", Opt. Lett., Vol. 24, No. 22, Nov. 15, 1989.

*Chapter 4*

4.1 Model 3900 CW Ti:Sapphire Laser Instruction Manual, Spectra Physics, 1250 W. Middlefield Rd., P.O. Box 7013, Mountain View, CA 94039.

4.2 C. Hovater and M. Poelker, "An Injection Modelocked Ti-Sapphire Laser for Synchronous Photoinjection", Proceedings of the 1997 Particle Accelerator Conference, Vancouver B. C., May 1997, to be published.

4.3 A. J. Alfrey, "Modeling of Longitudinally Pumped CW Ti:Sapphire Laser Oscillators", IEEE J. Quantum Electron., Vol. 25, pp. 760 – 766, No. 4, April 1989.

4.4 J. Kafka, A. Alfrey, and T. Baer, "Mode-locked continuous wave Titanium Sapphire Laser", in Ultrafast Phenomena VI, Berlin: Springer, 1988 pp64-65.

4.5 N. Sarukura and Y. Ishida, "Ultrashort Pulse Generation from a Passively Mode-Locked Ti:Sapphire Laser Based System", IEEE J. Quantum Electron., Vol. 28, No. 10 Oct. 1992.

4.6 P.T. Ho, in Picosecond Optoelectronic Devices, edited by C. H. Lee (Academic, New York, 1984).

4.7 "Laser Diode Operator's Manual and Technical Notes", SDL, Inc., 80 Rose Orchard Way San Jose, CA 95134-1365, 1994.

4.8 M. Poelker, Unpublished data, 1995.

*Chapter 5*

5.1 P. O'Shea, "Jitter Sensitivity in Photoinjectors," Proceedings of the 1995 Particle Accelerator Conference, Dallas Texas, May 1995.

5.2 M. Rodwell, D. Bloom, and K. Weingarten, " Subpicosecond Laser Timing Stabilization", IEEE J. Quantum Electron., Vol. 25, No. 4 April 1989.

5.3 "Phase noise characterization of microwave oscillators, phase detector method," Product note:11729B-1, Hewlett-Packard Co., P.O. Box 10301, Palo Alto, CA 94303.

5.4 U. L. Rhode, J. Whitaker and T.T.N. Bucher," Communications Receivers: Principals and Design," McGraw-Hill, 1997, pp. 344 – 362.

5.5 A. L. Lance, W. D. Seal and F. Labaar, "Phase Noise and AM Noise Measurements in the Frequency Domain," Infrared and Millimeter Waves, Vol. II, Academic Press, 1984, pp. 239 – 287.

5.6 S. Benson and M. Shinn, "Development of an Accelerator-Ready Photocathode Drive Laser at CEBAF", Proceedings of the 1995 Particle Accelerator Conference, Dallas Texas, May 1995.

5.7 D. B. Leeson "A Simple Model of Feedback Oscillator Noise Spectrum," Proc. IEEE, vol. 54 no 2, February 1966, pp. 329 – 330.

*Chapter 6*

6.1 M. Poelker, "High power gain-switched diode laser master oscillator, and amplifier", Appl. Phys. Lett. 67(19), 6 Nov. 1995.

6.2 A. J. Alfrey, "Modeling of Longitudinally Pumped CW Ti:Sapphire Laser Oscillators", IEEE J. Quantum Electron., Vol. 25, pp. 760 – 766, No. 4, April 1989.

6.3 J. Kafka, A. Alfrey, and T. Baer, "Mode-locked continuous wave Titanium Sapphire Laser", in Ultrafast Phenomena VI, Berlin: Springer, 1988 pp. 64-65.

6.4 J. A. Squier, "Development of High Average Power Femtosecond Chirped Pules Amplification Sources Using Chromium, Neodymium, and Titanium doped Materials", Ph.D. Dissertation, 1992 University of Rochester, Rochester NY. pp. 41 – 44.

6.5 E.P. Ippen and C. V. Shank, "Ultrashort Light Pulses", ed. S. L. Shapiro, Springer-Verlag, 1977, pp. 83-92.

6.6 "FR-103XL Autocorrelator Instruction Manual", 2123 4th Street, Berkeley, CA 94710, May 1996.

6.7 A. E. Siegman, "Lasers," University Science Books, Mill Valley, CA, 1986, Ch. 24, 27 and 29.

6.8 Model 3900 CW Ti:Sapphire Laser Instruction Manual, Spectra Physics, 1250 W. Middlefield Rd., P.O. Box 7013, Mountain View, CA 94039.

# APPENDIX A

# MIXER (PHASE DETECTOR) MATH

Figure 5.1 shows a typical phase detection scheme using a mixer [5.3]. We can represent the reference source and the frequency source signals by

$$V_R(t) = V\cos(\omega_R t) \text{ and } V_O(t) = V\cos(\omega_O t + \phi(t)) \qquad (A.1)$$

where V is the peak voltage of the signals, $\omega_R$ is the reference frequency, $\omega_O$ is the frequency source, and $\phi(t)$ is the phase modulation (noise) of the frequency source.
The output of the mixer is the product of the two signals given by [5.3]

$$V_{IF}(t) = KV\cos[(\omega_R - \omega_O)t + \phi(t)] + KV\cos[(\omega_R + \omega_O)t + \phi(t)] + \text{H.O. terms..} \qquad (A.2)$$

The low pass filter, in Figure 5.1, removes the higher frequency components leaving

$$V(t) = KV\cos[(\omega_R - \omega_O)t + \phi(t)] \qquad (A.3)$$

where K is the mixer efficiency. When operating the mixer as a phase detector the input signals must be at the same frequency, i.e. $\omega_R = \omega_O$, and $90^\circ$ out of phase, i.e. $\phi(t) = \Delta\phi(t) + 90^\circ$. Substituting this back into equation A.3 the mixer output is

$$\Delta V(t) = {}^{+}\text{-}\, KV\sin\Delta\phi(t) \qquad (A.4)$$

where $\Delta V(t)$ is the instantaneous voltage fluctuations around 0 Vdc and $\Delta\phi(t)$ is the instantaneous phase fluctuations. For $\Delta\phi(t) << 1$ radian, $\sin\Delta\phi(t) \sim \Delta\phi(t)$, then equation A.4 becomes

$$\Delta V(t) = {}^{+}\text{-}\, KV\Delta\phi(t) \qquad (A.5)$$

This is a linear relationship between the voltage fluctuations at the mixer output and the phase fluctuations of the input signals. KV is the phase detector constant (volts/radians), which is equal to the slope of the mixer sine wave output at the zero crossings.

It is typically more useful to view the phase detector output in the frequency domain. The output of the mixer as a function of frequency will be directly proportional to the input phase deviations, such that equation A.5 becomes

$$\Delta V(f) = KV\Delta\phi(f) \qquad (A.6)$$

Measuring the rms value on a audio spectrum analyzer and solving for $\Delta\phi_{rms}(f)$ gives

$$\Delta\phi_{rms}(f) = \Delta V_{rms}(f)/KV \qquad (A.7)$$

Equating A.7 with the spectral density defined in Chapter 5 as

$$S_{\Delta\phi}(f) = \frac{\Delta\phi^2{}_{rms}}{\text{Bandwidth}} \quad \text{rad}^2/\text{Hz} \qquad (5.1)$$

allows one to equate the spectrum analyzer output to the spectral density of phase fluctuations and determine the oscillator's phase noise.